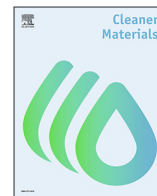


AUS Repository

Influence of nano-TiO₂, nano-Fe₂O₃, nanoclay and nano-CaCO₃ on the properties of cement/geopolymer concrete

Item Type	Article;Peer-Reviewed;Published version
Authors	Abdalla, Jamal A.;Thomas, Blessen Skariah;Hawileh, Rami A.;Yang, Jian;Jindal, Bharat Bhushan;Ariyachandra, Erandi
Citation	Abdalla, J. A., Thomas, B. S., Hawileh, R. A., Yang, J., Jindal, B. B., & Ariyachandra, E. (2022). Influence of nano-TiO ₂ , nano-Fe ₂ O ₃ , nanoclay and nano-CaCO ₃ on the properties of cement/geopolymer concrete. Cleaner Materials, 4, 100061. https://doi.org/10.1016/j.clema.2022.100061
DOI	10.1016/j.clema.2022.100061
Publisher	Elsevier
Rights	Attribution 4.0 International
Download date	2026-03-08 23:33:28
Item License	http://creativecommons.org/licenses/by/4.0/
Link to Item	https://hdl.handle.net/11073/26270



Influence of nano-TiO₂, nano-Fe₂O₃, nanoclay and nano-CaCO₃ on the properties of cement/geopolymer concrete



Jamal A. Abdalla^{a,*}, Blessen Skariah Thomas^{a,b,c}, Rami A. Hawileh^a, Jian Yang^{b,c,d}, Bharat Bhushan Jindal^e, Erandi Ariyachandra^f

^a Department of Civil Engineering, College of Engineering, American University of Sharjah, 26666, United Arab Emirates

^b Shanghai Key Laboratory for Digital Maintenance of Buildings and Infrastructure, School of Naval Architecture, Ocean and Civil Engineering, Shanghai Jiao Tong University, Shanghai 200240, PR China

^c State Key Laboratory of Ocean Engineering, Shanghai Jiao Tong University, Shanghai 200240, PR China

^d School of Civil Engineering, University of Birmingham, Birmingham B15 2TT, UK

^e School of Civil Engineering, Shri Mata Vaishno Devi University, Katra, Jammu & Kashmir, India

^f School of Built Environment, Western Sydney University, Penrith, NSW 2751, Australia

ARTICLE INFO

Keywords:

Sustainability
Supplementary cementitious material
Nanomaterials
Nano-TiO₂
Nano-Fe₂O₃
Nanoclay/metakaolin
Nano-CaCO₃
Geopolymer concrete

ABSTRACT

In past decades, researchers have tried to improve the durability of concrete by integrating supplementary cementitious materials into concrete. Recent advancements in the field of nano-engineered concrete have reported that nanomaterials significantly improve the mechanical and durability properties of concrete. This paper provides a comprehensive summary of recent developments on the use of nanomaterials as a performance enhancer in cement/geopolymer concrete. Many significant correlations associated with the reinforcement of cementitious matrices using nano-TiO₂, nano-Fe₂O₃, nanoclay/metakaolin, and nano-CaCO₃ were studied. Performance aspects such as fresh properties, microstructure, mechanical and durability characteristics, and the influence of various particle sizes have been reviewed. The findings from this review confirm the feasibility of using the nanomaterials in cement concrete, with the required properties of building materials. It is also expected that this review provides better insight into using nanomaterials in concrete for the benefit of academic and fundamental research and promotes its practical application in the construction industry.

Contents

1. Introduction	2
2. Scope of the literature review	2
3. Nanomaterials in cement/geopolymer concrete	3
3.1. Nanoclay	3
3.1.1. Effect of nanoclay on the properties of concrete	3
3.2. Nano-CaCO ₃	5
3.2.1. Effect of nano-CaCO ₃ on the properties of concrete	5
3.3. Nano-Fe ₂ O ₃	7
3.3.1. Effect of nano-Fe ₂ O ₃ on the properties of concrete	7
3.4. Nano-TiO ₂	9
3.4.1. Effect of Nano- TiO ₂ on the properties of concrete	10
4. Combinations of various nanomaterials	12
5. Discussion	12
6. Comparison of property enhancements among nanomaterial additives	12

* Corresponding author.

E-mail address: jabdalla@aus.edu (J.A. Abdalla).

Nomenclature

Abbreviations

C-A-H	Calcium-aluminate-hydrate
C-A-S-H	Calcium-aluminate-silicate-hydrate
C-S-H	Calcium-silicate-hydrate
CNT	Carbon nanotube
EDS	Energy-dispersive X-ray spectra
GO	Graphene oxide
ITZ	Interfacial transition zone
NA	Nano-aluminum oxide (nano-Al ₂ O ₃)
NC	Nanoclay
NF	Nano-hematite (nano-Fe ₂ O ₃)
NS	Nano-silicon dioxide (nano-SiO ₂)

NT	Nano-titanium dioxide (nano-TiO ₂)
NZ	Nano-zinc peroxide (nano-ZnO ₂)
RA	Recycled aggregate
RHA	Rice husk ash
SCC	Self-compacting concrete
SCM	Supplementary cementitious material
SEM	Scanning electron microscopy
UHPC	Ultra high-performance concrete
UPV	Ultrasonic pulse velocity
w/b	Water to binder ratio
wt%	Weight percentage
XRD	X-ray diffraction

7. Conclusions	13
Acknowledgments	15
References	15

1. Introduction

Ordinary Portland cement, produced at around 4–5 billion tons annually, is the costliest ingredient in cement concrete. It has been estimated that one ton of cement was produced per year for every human being (Andrew, 2018). The annual global production rate of concrete has been estimated to be 25–30 billion tons, and it is responsible for 8%–9% of the global anthropogenic greenhouse gas emissions. Reducing CO₂ emissions has attained prime importance around the globe, and minimizing Portland cement consumption has been identified as a major factor towards this goal. The need for high-strength concrete propelled the demand for higher cement content, further increasing greenhouse gas emissions. However, research in using nanomaterials to improve cement-based materials' mechanical and durability properties has gained significant momentum. The partial replacement of Portland cement with nanomaterials such as carbon nanotubes (CNTs), nano-SiO₂ (NS), nano-Al₂O₃ (NA), graphene oxide (GO), nano-TiO₂ (NT), nanoclay (NC), nano-ZnO₂ (NZ), nano-CaCO₃, and nano-Fe₂O₃ (NF) reduces carbon dioxide liberation while enhancing the mechanical and durability characteristics of concrete (Sumesh et al., 2017; Norhasri et al., 2017).

The increasing demand for ultra-high-performance concrete (UHPC) in the early millennium paved the way for nanotechnology application in cement concrete. Nano-engineered concrete has been developed as an alternative to silica fume concrete (which was conventionally used in the production of UHPC for better strength and durability) because of its limited availability and high cost. Nano-silica was first designed to mimic the characteristics of silica, which later led to the utilization of various other nanomaterials in cement-based materials (Norhasri et al., 2017; Sumesh et al., 2017).

Nano-science and engineering in concrete technology deal with the characterization of the nano-scale structure of cementitious materials and analyze how it influences macro-scale performance. Nano-engineered concrete can be fabricated by incorporating nanomaterials or nanotubes to achieve controlled novel properties. These properties include self-cleansing, healing and sensing capabilities, enhanced mechanical properties, high electrical resistivity, and better resistance to chloride, sulfate, and acid media (Sanchez and Sobolev, 2010). Nanomaterials significantly influence the mechanical properties because of their filler effects, high pozzolanic activity, nucleation effects, and nanoparticle size. The optimal quantity improves the prop-

erties significantly, while excess inclusion can cause agglomeration and negatively affect the concrete (Heikal and Ibrahim, 2016; Sadeghi-Nik et al., 2017). The following subsections explain the production methods and applications of commonly used nanomaterials.

2. Scope of the literature review

The foremost aim of this literature review is to access and evaluate the published literature on the influence of various nanomaterials, including nano-TiO₂, nano-Fe₂O₃, nanoclay/metakaolin, and nano-CaCO₃. The survey addresses the fresh properties, microstructure, mechanical, and durability characteristics, exploring the latest research developments. Four nanomaterials are commonly used in different studies, and their optimum dosages are identified and given in Fig. 1. The comparison of the physical properties of the four nanomaterials considered in the current study is provided in Table 1. The influences of various types of nanomaterials on the attributes of concrete are critically reviewed in the following paragraphs. Comparisons of the properties and performance of concrete using different nanomaterials are given, followed by a summary and conclusion.

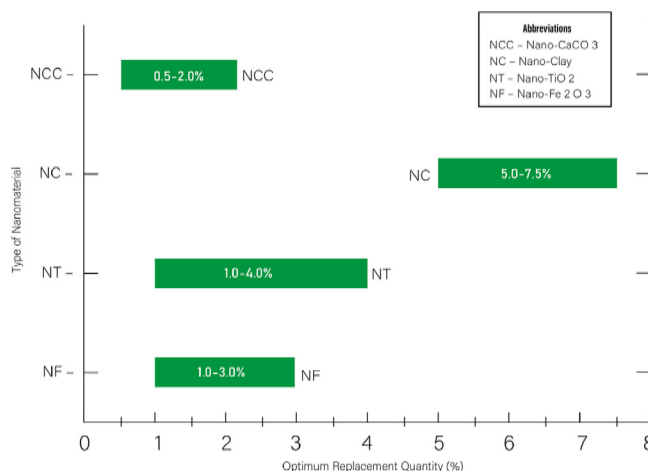


Fig. 1. Optimum replacement percentages of various nanomaterials.

Table 1
Physical properties of various nanomaterials considered in the current study.

Material	Purity	Average particle size	Specific surface area m ² /g	Density	Volume density	Appearance	Color	Reference (internet reference excluded)
Nano-TiO ₂	≥ 99.9 wt%	20 nm	>200	3.9 g/cm ³	0.35 g/cm ³	Spherical	White	Nikbin et al., (2019)
Nano-Fe ₂ O ₃	98.9	20 ± 5 nm	68	2.5 g/cm ³	0.5–1.20 g/cm ³	Spherical	Brown to orange	Abo-El-Enein et al (2018)
Nano-clay	99.9	176 nm	48–140.792	2.6 g/cm ³	0.25–0.68 g/cm ³	Tetrahedron	Off-white	Zhan et al., (2020)
Nano-CaCO ₃	≥ 98	20–110 nm	15–40	2.93 g/cm ³	0.4–0.68 g/cm ³	Cubic or hexagonal	white	Bankir et al., & Assaedi et al., (2020)

3. Nanomaterials in cement/geopolymer concrete

3.1. Nanoclay

Clays are fine-grained rocks/soil having limitless applications because of their physical and chemical attributes. Since prehistoric times, clays have been used in ceramics, agriculture, pottery, chemicals, construction materials, and civil engineering applications (Moreno-Maroto and Alonso-Azcárate, 2018). According to sedimentologists, clay particles are less than 4 μm, while geologists use 2 μm and colloidal chemists use 1 μm as the criterion (Guggenheim and Martin, 1995). Nanoclays are crystal-lattice-layered mineral silicates consisting of two-dimensional 1-nm-thick layers made up of two tetrahedral silica sheets fused to an edge-shaped octahedral sheet of alumina or magnesia. (Giannelis et al., 1999; Huang, 2018; Bergaya and Lagaly, 2013). Clay nanocomposites are in the smectite family of clays and have gained wide attention due to their low cost, wide availability, improved gas barrier, and mechanical and thermal characteristics.

Recently, nanoclays have been widely utilized in cement-based materials as a nanofiller due to their average particle size, roughly 1000 times finer than cement grains. Commonly used nanoclays are nano-kaolin [Al₂Si₂O₅(OH)₄] and nano-montmorillonite [(Ca,Na)_{0.3}Al₂(Si, Al)₄O₁₀(OH)₂]. Nano-halloysite [Al₂Si₂O₅(OH)₄] is a new type of nanoclay similar to kaolin with a hollow nanotube crystal morphology (Giannelis et al., 1999; Ghodke et al., 2016; Varga, 2007; Farzadnia et al., 2013a; Pique and Vazquez, 2013). Nanoclay can be considered a pozzolanic material because its major components are silica (44.98%–47.8%) and alumina (35.3%–41.8%), accounting for over 70% of the total composition.

In nano-metakaolin, silica varies from 45.5% to 89.6% and alumina from 18.9% to 42.3%, respectively. It can react with calcium hydroxide leading to the formation of C-S-H and C-A-H gels which can improve the mechanical and durability properties of the cementitious matrices (Niu et al., 2021; Zhan et al., 2020). Calcination of nanoclay at 600–800 °C results in the curtailment of the particle size leading to crystal structure destruction and amorphous phase formation, and the product is known as nano-metakaolin (Shebl et al., 2009; Jiang et al., 2019). The temperature for calcination plays a vital role in enhancing the reactivity of nanoclay. The optimum temperature for calcination of nano-halloysite and metakaolin was identified as 750 °C to obtain the best pozzolanic activity (Abo-El-Enein et al., 2014; Allalou et al., 2019).

Incorporating nanoclay and metakaolin (calcined nanoclay) can enhance the hydration process of cement-based materials. It was noted by Fan et al. (2015) that the increase in the quantity of nanoclay gradually reduced the quantity of calcium hydroxide, while the X-ray diffraction (XRD) peaks of C-S-H notably increased. Similarly, Hakamy et al. (2015) noted a decrease in calcium hydroxide from 16.8% to 12.1%, while the amorphous phases increased from 70.1% to 74.8%. It was noted by Heikal and Ibrahim (2016) that the incorporation of 6% calcined nanoclay increased the quantity of chemically combined water by 35%, 33%, 34%, and 29% at 3, 7, 28, and 90 days, respectively, while an excess of nanoclay can cause agglomeration, reduce the quantity of combined water, and hinder the hydration pro-

cess. XRD and scanning electron microscope (SEM) images of nanoclay are shown in Fig. 2.

The microstructure of the cementitious mixture is improved by adding nanoclay and calcined clay. Fan et al. (2016) observed that the addition of 1% nanoclay generated a surplus quantity of needle-like and fibrous C-S-H that intermixed to form a uniform and dense microstructure. The individual C-S-H crystals, ettringite, and loose C-S-H gels were not visible as they were in the control cement mortar samples. The pore structure of cement paste was refined on account of the pozzolanic and filler effect of the nanoclay. Fan et al. (2014) observed that incorporating 1% nanoclay reduced the total porosity by 19% and the average pore size by 21%. Similar observations by Fan and Zhang (2014) stated that the hydration reaction of calcined clay is much higher than the non-calcined types. The porosity of concrete containing 1%, 3%, and 5% calcined clay was reduced by 97%, 98%, and 89%, respectively, compared with the control concrete.

3.1.1. Effect of nanoclay on the properties of concrete

The workability of cement-based materials decreases when adding both calcined and non-calcined nanoclays and is significantly affected by higher dosages. As noted by Fan et al. (2014), the water required for standard consistency increases gradually to 133.25, 147.11, 149.07, 154.11, 157.85, and 162.07 kg with the incorporation of 0%, 1%, 3%, 5%, 7%, and 9% nanoclay, respectively, on account of its high specific surface area. The inclusion of 9% nano-metakaolin reduced the concrete slump by 15.7% (Norhasri et al., 2016). Similarly, Heikal and Ibrahim (2016) noted that adding 1%, 4%, and 8% calcined nanoclay reduced the initial setting time by 5%, 11%, and 24%, respectively, while the final setting time was reduced by 9%, 16%, and 22% respectively.

Nanoclay and calcined nanoclay significantly influence the mechanical properties because of high pozzolanic activity, nucleation effects, and nanoparticle size. The optimal quantity improves the properties significantly, while excess inclusion can negatively affect the concrete. Excess nanomaterials can agglomerate, hindering the hydration process while also incapacitating the bonds between the aggregate and cement matrix (Liao et al., 2004; Heikal and Ibrahim, 2016; Sadeghi-Nik et al., 2017). Ultrasonic dispersion can disintegrate the agglomeration as mentioned by Hamed et al. (2019), who noted an enhancement in the compressive, tensile, and flexural strength by 52%, 28%, and 35%, respectively, in contrast with 18%, 10%, and 15% (non-ultrasonic treated nanoclay) at a 7.5% dosage.

Nano-metakaolin exhibited little influence on the early strength characteristics of ultra-high performance concrete (Norhasri et al., 2016). It was noted by Morsy et al. (2014) that the compressive strength was enhanced by 15%, 34%, and 19%, and the flexural strength by 6%, 29%, and 19% with the addition of 2.5%, 7.5%, and 10% calcined nanoclay (nano-metakaolin), respectively. A similar observation by Hakamy et al. (2015a) noted that calcined nanoclay provides compressive strength increased by 39%, 35%, and 26% when compared to the 31%, 23%, and 17% (of the normal nanoclay), respectively, at 1%, 2%, and 3% dosages. The optimal dosage for non-calcined nanoclay was observed to be around 5%–7.5%, while that of the calcined nanoclay was between 0.5% and 2%. The compressive strength of the mortar specimens having 6% nano-metakaolin

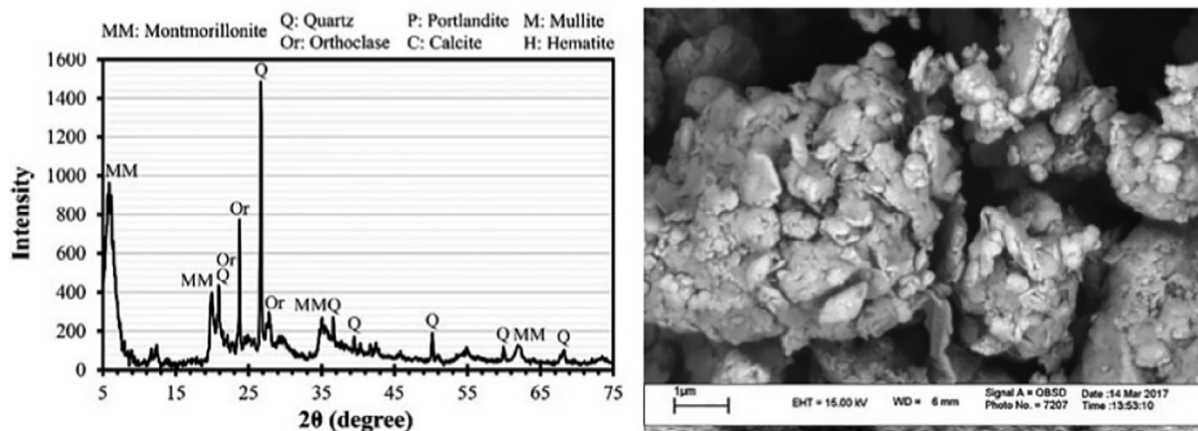


Fig. 2. a) X-ray diffraction, and b) scanning electron microscope images of nanoclay (Langaroudi et al., 2019).

increased by 11% at 28 days, while the combination of 6% nano-metakaolin and 0.02% carbon nanotubes improved it by 29% because of the bridging effect and better dispersion of nanomaterials.

The toughness and elastic modulus of nanoclay concrete was investigated by various researchers. Langaroudi et al. (2018) added 3% nanoclay to four types of concrete individually, including 15% silica fume, 45% blast furnace slag, 15% rice husk ash, and 30% fly ash, partially substituting the binder by weight. It was noted that the inclusion of 3% nanoclay improved the elastic modulus respectively by 0.8%, 2%, 5.4%, and 7.7% when compared to the control blends. The elastic modulus of the reactive powder concrete improved by 12.27%–21.88% with the incorporation of 2%–5% nano-metakaolin (Habeeb et al., 2019). Similar research by Alharbi et al. (2021) pointed out a 25% increment in the elastic modulus when 3% calcined clay was added to a reactive powder concrete. According to research published by Hakamy et al. (2015a), the fracture toughness of concrete was enhanced by 31% when incorporating 1% nanoclay and by 40% when incorporating 1% calcined clay. Another study by Hakamy et al. (2015) noted a 38% enhancement in fracture toughness with the utilization of 1% calcined nanoclay because of its pozzolanic activity and pore-filling effect.

Langaroudi et al. (2018) noted a reduction in the water absorption and penetration of concrete when it included 1%, 2%, and 3% nanoclay. The initial water absorption was trimmed by 60.4%, 40.6%, and 65.6%, respectively, while the final water absorption was correspondingly reduced by 20.2%, 11.0%, and 53.2%. When 3% nano clay was added to the four types of concrete individually, including 15% silica fume, 45% blast furnace slag, 15% rice husk ash, and 30% fly ash partially substituting the binder by weight, the final water absorption was reduced by 47.8%, 30.91%, 7.5%, and 11.32%, respectively. The water penetration of concrete that included 1%, 2%, and 3% nanoclay decreased by 42.9%, 42.9%, and 64.3%, respectively, compared to the control specimen. Ibrahim (2013) observed similar results, reporting 16.6%, 21.79%, and 25.6% improvements respectively when including 3%, 5%, and 10% nano-metakaolin.

Langaroudi et al. (2018) measured an enhancement in the electrical resistivity of concrete when including nanoclay. The electrical resistivity of specimens incorporating 1%, 2%, and 3% (at 90 days of curing) was enhanced by 122.1%, 96.7%, and 189%, respectively, caused by the reduction of interconnecting pore structures by the pozzolanic reactivity of the nanoclay. Langaroudi and Mohammadi (2018) observed severe scaling and surface deterioration of a control specimen after 150 cycles of freeze and thaw, while the nanoclay specimens were slightly scaled and less affected. The 300 freeze–thaw cycles led to a drastic deterioration in the control specimen; however, the nanoclay specimen was less severely affected. The control concrete exper-

rienced 18.64% mass loss, 72% compressive strength loss, and a 45% reduction in the dynamic modulus of elasticity. Concrete incorporating 1%, 2%, and 3% nanoclay underwent 13.14%, 9.0%, and 3.96% mass loss; 47%, 52%, and 30% compressive strength loss; and 28.5%, 25.3%, and 15.5% reductions in the dynamic modulus of elasticity, respectively. Similar results were also observed by Fan et al. (2015).

Resistance to acid attack was investigated by Fan et al. (2016), who reported a 17% reduction in the compressive strength with the incorporation of 3% nanoclay after 60 days of exposure (Fig. 3). Similar studies by Diab et al. (2019) pointed out that the compressive strength loss, weight loss, and ultrasonic pulse velocity (UPV) were reduced respectively by 20.1%, 18.9%, and 31.2% for the 3% calcined nano clay concrete when compared with the control specimen after 150 days of exposure in sulfuric acid solution. Concrete specimens incorporating 1%, 3%, 6%, and 9% nano-metakaolin reduced the weight loss caused by magnesium sulfate attack by 11.4%, 20.7%, 32.5%, and 41.4%, respectively, and the expansion strain was reduced by 4.9%, 17.0%, 21.3%, and 26.0%, respectively, when compared with the control specimen.

Some researchers investigated the resistance of nanoclay concrete to chloride penetration, concluding that nanoclay-incorporated and calcined nanoclay-incorporated concrete is highly resistant. He and Shi (2008) pointed out that the chloride diffusion coefficient of mortars incorporating 1% hydrophilic nano-montmorillonite (clay-hi) and hydrophobic nano-montmorillonite (clay-ho) was reduced by 66% and 76%, respectively, when compared with the control mortar. Guo et al. (2018) pointed out that the chloride permeability coefficient of mortar containing 4% nano-metakaolin improved by 18.93%–31.05% at 7–28 days compared to the reference specimen. Fan and Zhang (2014) noted that the chloride penetration reduced by 27%, 29%, 53%, 31%, and 23% respectively at nanoclay contents of 1%, 3%, 5%, 7%, and 9%. A similar observation by Langaroudi et al. (2018) noted the lowest chloride migration coefficient when 3% nanoclay was incorporated.

Shrinkage in nanoclay concrete may vary with different nanoclay types because their morphology and chemical compositions may notably influence it (Niu et al., 2021). It was demonstrated by Polat et al. (2015) that the autogenous shrinkage was reduced by 43% for mortar incorporating 1.3% nanoclay and by 40% for 3% nanoclay incorporation compared with the control specimen. A similar claim was made by Lee et al. (2018), who noted that the maximum crack width, average crack width, average crack length, and total crack area of mortar containing 0.25% nanoclay were respectively 23.9%, 41.9%, 48.8%, and 69.3% lower than for a control specimen.

The behavior of nanoclay concrete at high temperatures was investigated by Irshidat and Al-Saleh (2018). It was noted that the compres-

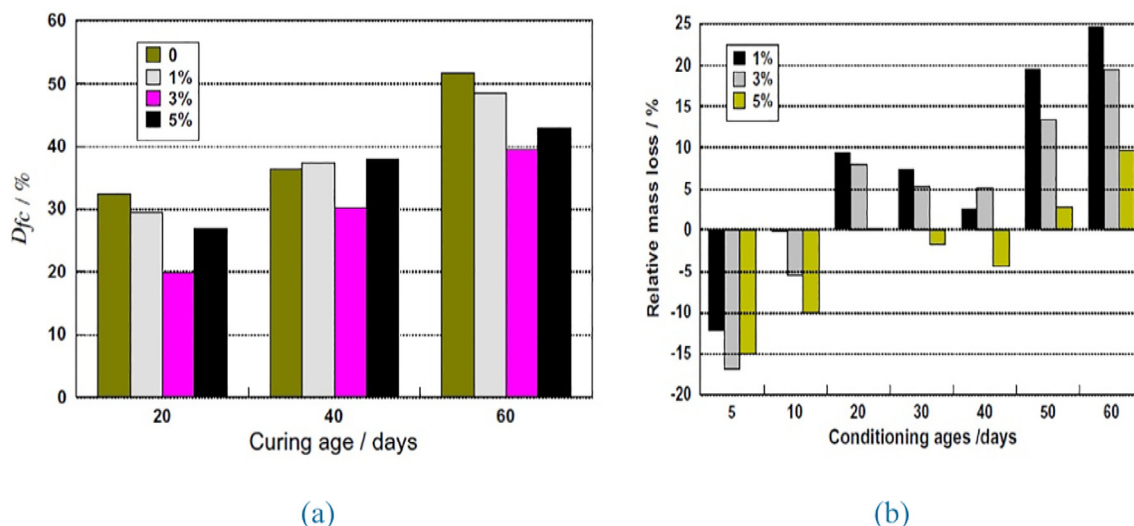


Fig. 3. (a) Compressive strength loss, (b) Mass loss of concrete with nanoclay after exposure to acid media (Fan et al., 2016).

pressive strength, tensile strength, and flexural strength improved for concrete containing 2% nanoclay after exposure to high temperatures (Fig. 4). At a temperature of 600 °C, the compressive strength, tensile strength, and flexural strength were enhanced by 15%, 27%, and 106% compared with a control specimen. Ghazy et al. (2015) noted an enhancement in the compressive strength of the concrete containing 5% and 10% nano-metakaolin by 1.56% and 11.55%, respectively, at 200 °C, while it was reduced by 42.71% and 30.56%, respectively, at 800 °C. Similar results were also noted by Al-Khafaji et al. (2016).

3.2. Nano-CaCO₃

Calcium carbonate (CaCO₃) is one of the most abundant and economically viable naturally occurring minerals, extensively used by various industries as a filler material while also helping to improve some composite material mechanical characteristics. It is generally obtained from limestone, chalk, and marble and is also produced artificially by the reaction of Ca with CO₂. Mineral calcium carbonate is crushed, ground, sieved, and re-crystallized into nano-CaCO₃. The application of nano-CaCO₃ lies broadly in paints, paper making, sealants, medicine, plastics, and the food industry (Pera et al., 1999; Lin et al., 2008; Souza et al., 2008; Yang et al., 2020).

The use of micro-limestone mainly enables the filler effect, densifying the microstructure. Nano-limestone can accelerate the hydration of cementitious materials because of nucleation effects and filler characteristics (Lothenbach et al., 2008; Kumar et al., 2013; Li et al., 2016). It was pointed out by Batuecas et al. (2021) that the incorporation of 2% nano-CaCO₃ into cement reduces the CO₂ content. Traditional Portland cement contained 0.96 kg CO_{2-eq}/kg of cement, while Portland cement incorporating 2 wt% of nano-CaCO₃ had only 0.3 kg CO_{2-eq}/kg cement, a 69% reduction.

Wu et al. (2021) noted that the major constituents of nano-CaCO₃ are CaO and CO₂, at 54.77% and 43.3%, respectively (Fig. 5). Remaining constituents are 1.23% SO₃, 0.25% Fe₂O₃, 0.18% MgO, 0.12% SiO₂, and traces of Al₂O₃ and Na₂O at 0.09% and 0.06% respectively. Ca(OH)₂ has been used as a natural stabilizer for CaCO₃, enabling the production of rice-like hollow nano-CaCO₃ without any agglomeration (Ulkeryildiz et al., 2016). A high modulus at the interfacial transition zone (ITZ) around the coarse aggregate from the addition of NC was observed in a nano-indentation test, revealing that the pozzolanic reactions generated additional C-S-H gels (Hosan et al., 2021).

3.2.1. Effect of nano-CaCO₃ on the properties of concrete

The addition of 1% nano-CaCO₃ significantly reduced the volume of permeable voids by 46% after 28 days of curing. In the case of high

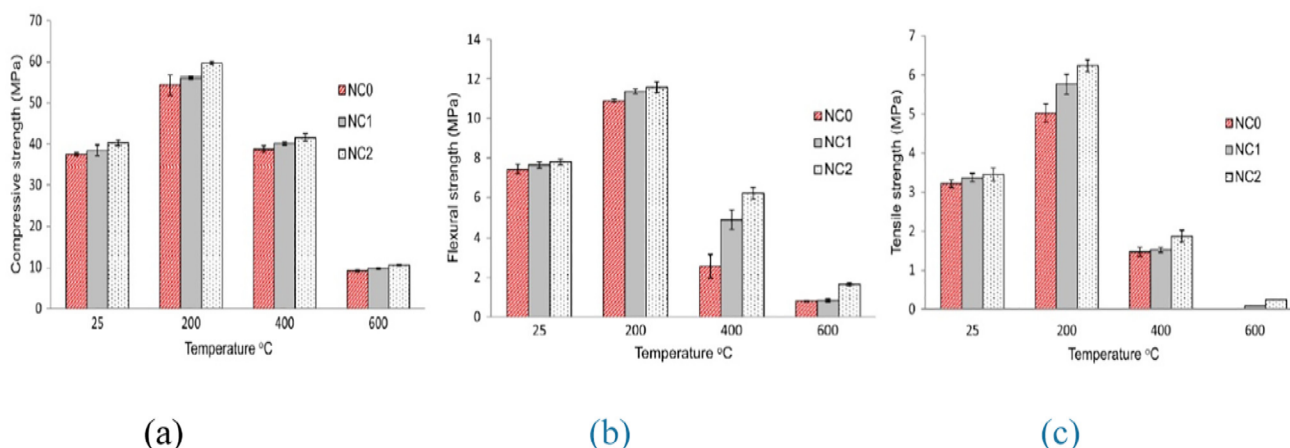


Fig. 4. Residual properties of nanoclay concrete: (a) compressive strength, (b) flexural strength, (c) tensile strength (Irshidat and Al-Saleh, 2018).

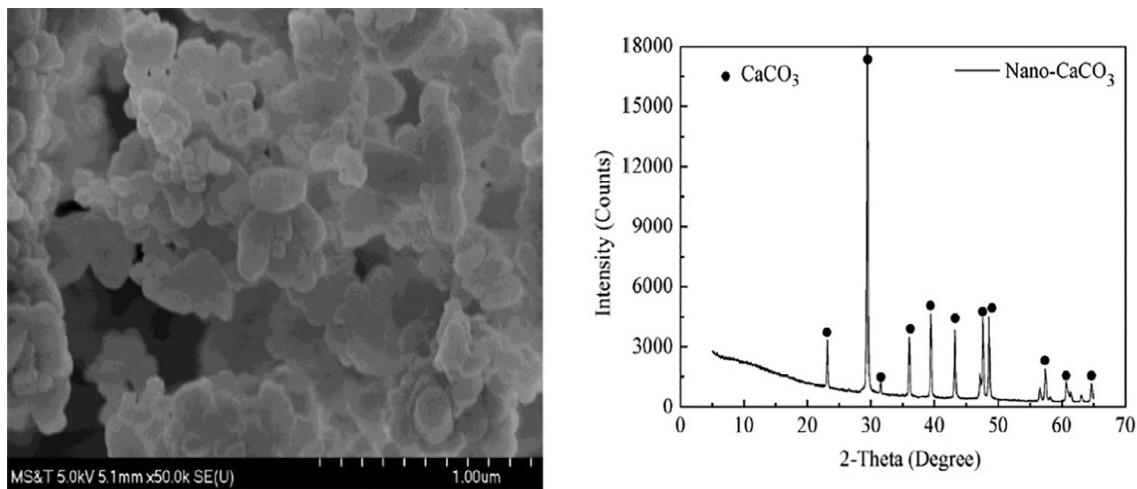


Fig. 5. a) SEM image, and b) XRD pattern of nano- CaCO_3 (Wu et al., 2021).

volume fly ash concrete (40%), the volume of permeable voids was reduced by 30% and 46%, respectively, at 28 and 90 days of curing (Shaikh and Supit, 2014). Wu et al. (2016) observed a reduction in porosity from 15.2% to 12.5% when the nano- CaCO_3 quantity was increased from 0% to 3.2%. Meanwhile, the porosity increased from 12.5% to 17.5% when the nano- CaCO_3 quantity increased from 3.2% to 6.4%. It was noted by Wu et al. (2016) that the heat of hydration was modified with the addition of NC. The control blend dormant period was observed to be around 13 h and was reduced to 9 h because of the chemical effects (dilution and nucleation) and pore-filling characteristics of the NC. Hosan and Shaikh (2020) did not observe significant changes in the calcium hydroxide peaks in high-volume slag pastes and high-volume slag fly ash paste containing NC during X-ray diffraction analysis. Enhanced intensity of ettringite, calcium aluminohydrate, calcium carbonate, and calcium silicate hydrate was observed.

Microstructural characteristics, as observed by mercury intrusion porosimetry, indicate that the addition of nanoparticles considerably reduces porosity (Ding et al., 2020). The cumulative mercury volume intruding in control concrete was $0.0412 \text{ cm}^3/\text{g}$, while that of the concrete including 1%, 2%, 3%, and 4% NC was 0.0365, 0.0254, 0.0189, and $0.0101 \text{ cm}^3/\text{g}$, respectively (Khotbehsara et al., 2018). Similar results were observed by Wu et al. (2018a), who noted that the porosity of the control specimen was 15.2%, which reduced to 12% with 3.2% of NC content. The incorporation increased the porosity by 17.5% for 4.8% NC and 18.3% for 6.4% NC, as high NC content may lead to agglomeration. The incorporation of NC refined the middle capillary pores (50–100 nm size), increasing the volume of mesopores (10–50 nm) by 60%.

The workability of concrete incorporating NC decreased with increasing content, as observed by Shaikh and Supit (2014). The slump value was reduced from 140 mm for the control blend to 135 and 120 mm, respectively, for mixtures containing 1% and 2% NC. Liu et al. (2012) noted that the initial and final setting times of the cementitious matrix gradually reduced with increasing nano- CaCO_3 content. The control blend's initial setting time, final setting time, and flowability were 200, 260, and 163 mm, respectively. These were reduced to 187, 232, and 137 mm for 1% nano- CaCO_3 ; 139, 221, and 130 mm for 2% nano- CaCO_3 ; and 130, 207, and 120 mm for 3% nano- CaCO_3 . In contradiction to the above findings, Camilletti et al. (2013) observed improved flowability with increased NC in an ultra-high performance concrete mix.

Wu et al. (2021) observed a 9% improvement in the compressive strength, a 20% improvement in flexural strength, and a 41% improvement in the bond strength when 3.2% nano- CaCO_3 was used. Li et al.

(2015, 2015a) noted that 3% is the optimum content, improving compressive strength by 3%–19% and flexural strength by 11%–28%. The pull-out strength improved by 200%, and the fiber-matrix bond strength improved by 45%, as observed by Wu et al. (2018). It was noted by Liu et al. (2012) that the optimum content of nano- CaCO_3 was 1%–2%. Beyond this level, the mechanical properties were reduced (Fig. 6). Maximum flexural strength (108.4% and 108.3% higher than control at 7 and 28 days, respectively) was observed for 1% nano- CaCO_3 , while the maximum compressive strength was noted at 2% NC (111.2% and 108.6% higher than control at 7 and 28 days, respectively). Similarly, Assaedi et al. (2020) noted improved flexural tensile strengths of 3.09, 4.30, and 4.21 MPa, respectively, for 1%, 2%, and 3% NC geopolymer concrete compared with 2.71 MPa for the control concrete. Similar results were also observed by Cosentino et al. (2020). Su et al. (2016) noted that ultra-high performance concrete incorporating 3% nano- CaCO_3 exhibited 60% higher splitting tensile strength than nano-silica concrete specimens.

The water sorptivity of mortars and concrete containing 1% NC experienced 19% and 60% reductions from the control at 28 and 90 days, respectively, as newly formed C-S-H gels filled the concrete capillary pores. The addition of NC densified the microstructure, enhancing the concrete density by refining the pores (Shaikh and Supit, 2014). The capillary water absorption of concrete containing 2% NC was reduced by 61% (Fig. 7), and 3% NC concrete gave the lowest water absorption (65%–70% improvement), as observed by Khotbehsara et al. (2018).

The shrinkage of a cementitious blend incorporating NC was studied by Liu et al. (2012). It was established that the early age shrinkage of cement paste incorporating 1% nano- CaCO_3 was only 1/3 that of the control paste, while it became twice the control when the NC content was 2%. Camilletti et al. (2013) noted 18% reduced shrinkage and 3% lower mass loss for specimens containing 5% NC. The resonance frequency increased with the addition of NC, as observed by Bankir et al. (2020), as 1% NC improved the resonance frequency by 10%. The resonance frequency of the control was 3012 Hz, whereas including 1% NC improved the resonance frequency to 3330 Hz, and 2% NC had a 3015 Hz resonance frequency. In contradiction to the results above, Li et al. (2016) pointed out that ultra-high performance concrete containing 2% NC with water to binder ratios of 0.15 and 0.18 exhibited 16% and 29% higher autogenous shrinkage than the control concrete. At 72 h, the autogenous shrinkage increased by 7.56% and 16.87% with 1% and 2% NC added. Similar results were also reported by Hosan and Shaikh (2021).

Shaikh and Supit (2014) noted that the chloride penetration charges passed through control concrete were respectively 3442 and

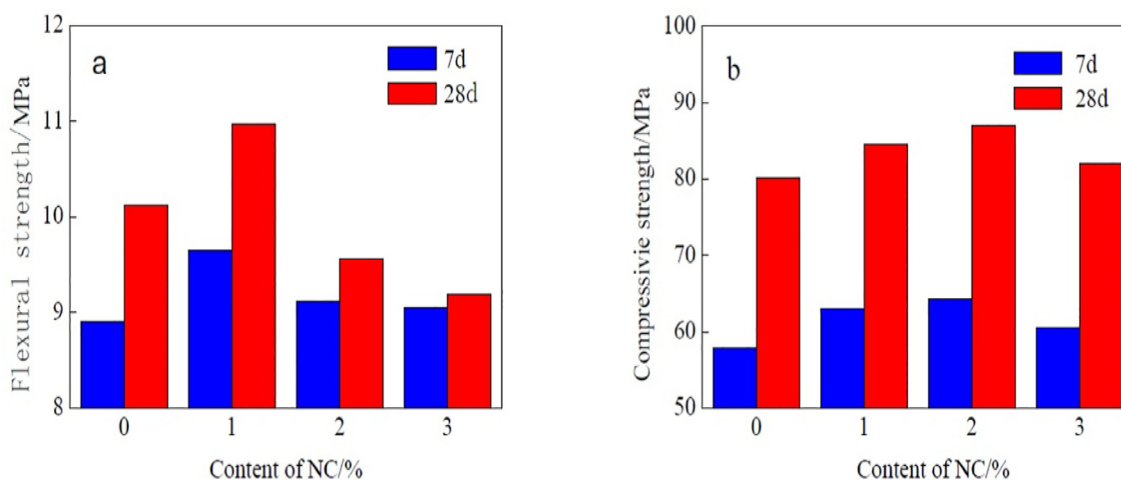


Fig. 6. a) Variation in flexural strength, and b) compressive strength of concrete with nano- CaCO_3 (Liu et al., 2012).

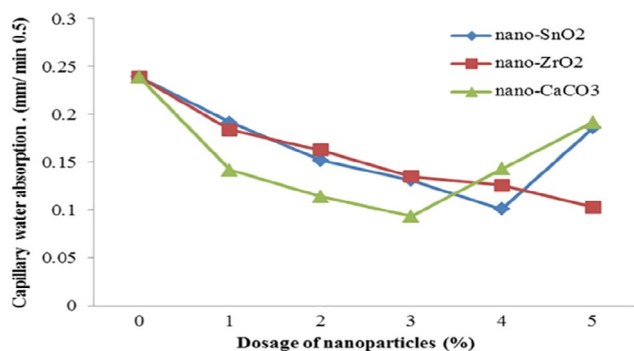


Fig. 7. Capillary water absorption of concrete containing various nanomaterials (Khotbehsara et al. 2018).

2916 C at 28 and 90 days. With the addition of 1% NC, the chloride penetrations were reported as 2749 and 1475 C, respectively, at 28 and 90 days, indicating corresponding improvements of 20% and 50%. The lower passed charges indicate high resistance to chloride penetration. The chloride diffusion coefficients of control and 1% NC concrete were 4.1×10^{-12} and 1.07×10^{-12} m^2/sec , respectively, about a 73% reduction. Shaikh and Supit (2015) further noted that chloride permeabilities at 28 and 90 days were reduced by 11.8% and 7.7%, respectively. By contrast, the chloride diffusion coefficient at 60 days was reduced by 32.6% compared with the control concrete (Herath et al., 2020).

The behavior of concrete subjected to acid attack was studied by Bankir et al. (2020), who reported that the mass loss of the control specimen after the acid attack was 7.8% compared with 5.3% for mortar containing 20% blast furnace slag (Fig. 8). With 1% NC, the mass loss was 3.6%. Khotbehsara et al. (2018) demonstrated that the electrical resistivity of a control concrete was very low, indicating a high possibility of corrosion. The control specimen resistivity was 7.2 $\text{k}\Omega\text{-cm}$, while that of the 4% NC concrete was 25 $\text{k}\Omega\text{-cm}$, an improvement of up to 257% compared to the reference.

Wu et al. (2016) studied properties at high temperatures, noting no obvious changes up to 450–550 °C. When the temperature was increased to 600–700 °C, decomposition of CaCO_3 was observed, which increased further with an increasing quantity of CaCO_3 . Salih et al. (2020) observed similar results while noting an 83% reduction in the sum of cement weight loss at 600–800 °C when 1% NC was incorporated. Bankir et al. (2020) observed that the thermal conductivity of a control mortar sample was 1.23 W/m-K , while that of sam-

ples containing 1% and 2% NC were 1.79 and 1.17 W/m-K , respectively. Including 20% blast furnace slag reduced the thermal conductivity to 1.01 W/m-K .

3.3. Nano- Fe_2O_3

Nano- Fe_2O_3 (NF), also known as nano-hematite, improves the properties of cement-based materials because of its nano-filling effect, better dispersion ability, acceleration of C-S-H formation, and porosity reduction. The investigations carried out by Li et al. (2004, 2004a) were the first reported in the literature on the use of nano- Fe_2O_3 (NF) particles in cement-based materials. It was identified that the cement mortar, when mixed with NF, turns into a smart structural material that can self-monitor the stress with improved diagnostic ability. The reaction between Fe_2O_3 and $\text{Ca}(\text{OH})_2$ leads to the formation of ilavite compound having void filling characteristics similar to ettringite (Amin et al., 2013). The reaction of nano-ferric oxide with calcium hydroxide generates nano-reinforcing materials that densify the concrete microstructure (Heikal et al., 2021). Concrete composite incorporating 2% NF exhibited the highest gamma radiation shielding capacity compared with ordinary Portland cement concrete (Abo-El-Enein et al., 2018); an energy-dispersive X-ray spectra (EDS) image is given in Fig. 9. The inclusion of NF facilitates additional nucleation sites for C-S-H, accelerating the growth of hydration products in the pores/voids within the concrete materials (Feng et al., 2020).

The addition of NF refines the pore structure and increases the viscosity of the cement matrix. The most probable pore diameter decreased from 14 nm in the control specimen to 13 nm for 3% NF and 11.9 nm for 4% NF. The median volume diameter improved from 22.2 nm for the control to 19.7 and 14.5 nm for 3% and 4% NF, respectively. The addition of up to 4% NF can accelerate the hydration of cement and enhance the rate of exhausted heat (Khoshakhlagh et al., 2012). NF acts as a filler and activates the cement hydration, reducing the $\text{Ca}(\text{OH})_2$ crystals. The large pores observed in the control specimen became filled in the NF-modified samples, making a compact microstructure indicating the rapid formation of C-S-H gels (Madandoust et al., 2015).

3.3.1. Effect of nano- Fe_2O_3 on the properties of concrete

The fresh properties of concrete incorporating NF were investigated by Madandoust et al. (2015). The control mixtures' slump and v-funnel flows were 24.5 cm and 8.5 s, respectively. The slump flow of concrete incorporating 1%, 2%, 3%, 4%, and 5% NF were respectively 24, 24, 24.5, 25 and 25.5 cm, while the v-funnel flow values were 9.4, 10.5, 9.8, 8.5 and 7.8 s. It was noted that the v-funnel flow

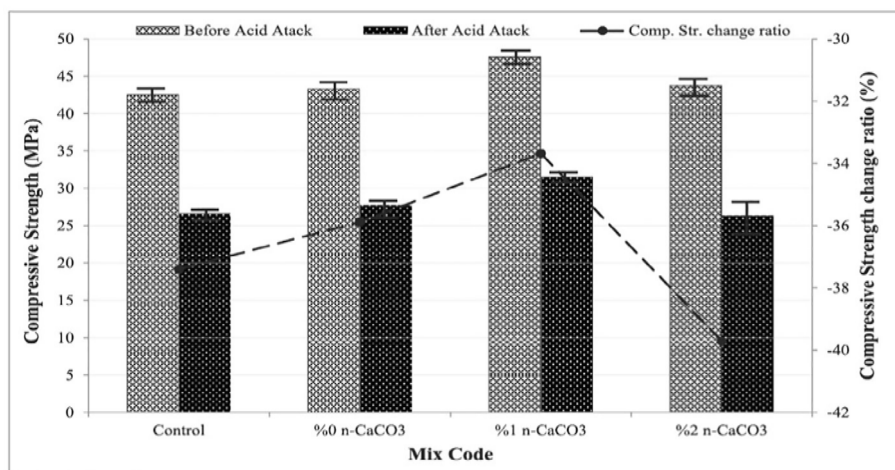


Fig. 8. Compressive strength of acid-attacked specimen before and after the acid attack (Bankir et al., 2020).

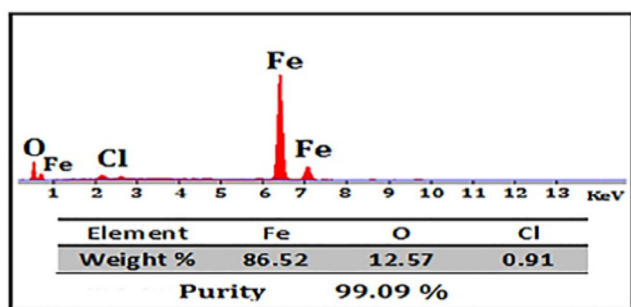


Fig. 9. EDS image of nano-Fe₂O₃ (NF) (Abo-El-Enein, 2018).

values gradually decreased with an increasing quantity of NF. Similar observations were made by Joshaghani et al. (2020), who noted improved v-funnel and l-box values for up to 3% NF in self-compacting concrete. Feng et al. (2020) noted a 34.5% increase in the slump flow with the incorporation of 2% NF, while the compressive and tensile strength substantially improved with 1% fiber, as shown in Fig. 10. Generally, the high surface area of the nanoparticles absorbs more water and increases the water demand in the mixture, requiring a high dosage superplasticizer (Joshaghani et al., 2020).

A significant reduction in microcracks and a compact microstructure was noted by Feng et al. (2020) when incorporating 2% NF distributed uniformly. While incorporating NF up to 2% provided an

excellent filling effect, exceeding 2% led to nanoparticle agglomeration, subsequent porosity enhancement, and quality degradation of the concrete. Including NF converts the loose needle-like microstructural particles of the binder materials to a compact integrated morphology, which can arrest cracks (Ghazanlou et al., 2020; Kani et al., 2021).

Li et al. (2004, 2004a) reported that compressive strength improved by 26% and 14.5% for the addition of 3% and 5% NF, respectively, while the flexural tensile strength improved by 17.8% and 23%, respectively. Oltulu and Şahin (2011) noted the compressive strength of control concrete as 65 MPa, while that of the concrete incorporating 0.5 wt%, 1.25 wt%, and 2.5 wt% NF was respectively 74.6, 67.6, and 69.4 MPa. Khoshakhlagh et al. (2012) noted the best compressive strength at 4% NF. The compressive strength of the control self-compacting concrete (SCC) was 31.6 MPa at 28 days (71.83% improvement), while that if the concrete incorporating 3% and 4% NF were 48.2 and 54.3 MPa, respectively.

Nazari and Riahi (2011) observed an increasing trend in the splitting tensile strength when incorporating nano-Fe₂O₃ (NF) particles. The splitting tensile strength of the water cured and lime water cured control specimens were respectively 2.3 and 1.9 MPa. The strengths of water cured specimens containing 0.5 wt%, 1 wt%, 1.5 wt%, and 2 wt % NF particles were respectively 2.7, 3.2, 3.0, and 2.3, while that of the lime water cured specimen were 3.0, 3.1, 3.3, and 3.9 MPa, respectively. Khoshakhlagh et al. (2012) noted a better performance of 3.1 MPa with 4% NF than the 1.6 MPa of the control specimen

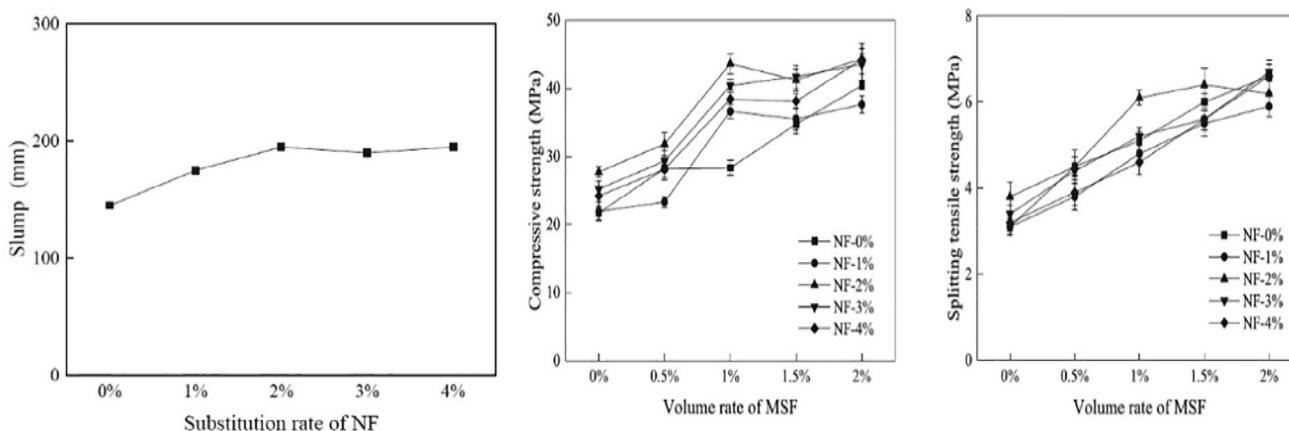


Fig. 10. a) Workability, b) compressive strength, and c) splitting tensile strength of NF concrete (Feng et al., 2020).

(93.75% improvement). [Khoshakhlagh et al. \(2012\)](#) also noted better flexural strength performance of 7.4 MPa with 4% NF when compared with the 4.2 MPa of the control specimen (76.19% improvement). The addition of 0.5% NF increased the strength by 24%, while the inclusion of 1 wt% improved it by 55% ([Nazari et al., 2010](#); [Oltulu et al., 2011](#)). Similar observations by [Kani et al. \(2021\)](#) noted flexural tensile strengths enhanced by 134%, 158%, and 142%, respectively, for specimens incorporating 2%, 3%, and 4% NF.

[Nazari and Riahi \(2011\)](#) observed a trend of water absorption reduction when incorporating the nano-Fe₂O₃ (NF) particles. The water absorption of the water cured and lime water cured control specimens were respectively 4.80% and 4.92%. The water absorption of water cured specimens containing 0.5%, 1%, 1.5%, and 2 wt% NF particles were respectively 0.92, 1.17, 1.40, and 1.71, while the corresponding values for the lime water cured specimens were 0.85, 0.95, 1.03, and 1.15, respectively. [Khoshakhlagh et al. \(2012\)](#) observed that the water absorption of the control specimen was 3.89%, while that of the specimens including 3% and 4% NF were 1.23% and 1.02%, respectively. The absorption decreased by 73.77% with 4% NF. Similar observations were made by [Joshaghani et al. \(2020\)](#), who noted a 64% reduction with 5% NF.

The capillary permeability of mortars containing NF was studied by [Oltulu and Şahin \(2011\)](#). It was noted that concrete capillary permeability incorporating 0.5 wt%, 1.25 wt%, and 2.5 wt% NF was reduced by 26%, 13%, and 6%, respectively. In comparison, the capillary permeabilities for mortars containing combined nano-silica and NF at 0.5 wt%, 1.25 wt%, and 2.5 wt% were reduced by 12%, 14%, and 17%, respectively. The probability of corrosion is reduced with an enhancement in the electrical resistivity. [Madandoust et al. \(2015\)](#) noticed a much lower electrical resistivity value of 7.2 kΩ-cm for the control specimen, which increased to the range of 18 (150%), 22 (214.3%), and 15.4 kΩ-cm (113.8%) with the inclusion of 1%, 2%, and 3% NF, respectively. Similar studies by [Joshaghani et al. \(2020\)](#) have pointed out a substantial increase in the electrical resistivity of concrete at 28 and 91 days, especially at lower water to binder (w/b) ratios.

The behavior of NF concrete subjected to sulfate attack was studied by [Heikal et al. \(2021\)](#), who utilized two types of NF (processed at 300 and 450 °C in an electric furnace for 2 h). As observed in [Fig. 11](#), the

compressive strength of specimens containing 0.5% and 1% NF (processed at 300 °C) was higher than that of the control concrete. All concrete specimens containing 450 °C NF (0.5%–2 wt%) were higher than the control specimens. The rapid chloride permeability of the control specimen was 2900 C, which was reduced by 44% with the inclusion of 2 wt% NF ([Madandoust et al., 2015](#)). [Braganca et al. \(2016\)](#) noted enhanced resistance to sulfate attack as nano-magnetite reacts with calcium hydroxide to form the Fe-ettringite phase that reduces porosity.

The behavior of NF mortar specimens at elevated temperatures of 110–650 °C was investigated by [Khoshakhlagh et al. \(2012\)](#), who noticed an enhanced weight loss for specimens containing NF. The control specimen underwent a 10.6% weight loss, while the specimens containing 3%, 4%, and 5% NF had respective weight losses of 11.7%, 11.6%, and 11.3%. In contradiction, [Abo-El-Enein et al. \(2018\)](#) reported that the NF concrete exhibited better performance when exposed to 600 °C temperatures. The compressive strength reduction was 20% and 18% (24% and 26% less) for the concrete containing 2% and 3% NF, respectively, compared with 44% for the control concrete. Greater reductions for NF concrete were noted at 800 °C, which were 73% and 74% for 2% and 3% NF, respectively, compared with 69% for the control concrete.

3.4. Nano-TiO₂

Nano-sized titanium dioxide (TiO₂), a semiconductor photocatalyst, is one of the most extensively investigated nanomaterials. The photo-catalysis characteristic of titanium dioxide was first identified by Fujishima and Honda. It splits water into hydrogen and oxygen by UV light energy-instigated electro-catalysis utilizing TiO₂ as a photo-anode in an electrochemical cell. This process is popularly known as the Honda-Fujishima effect ([Paul and Giri, 2018](#); [Sanalkumar and Yang, 2021](#)). Nano-TiO₂ (NT) is a versatile material widely used as the white pigment in paints and cosmetics, glass, wall-paper materials, cement-based materials, and ceramic tiles. Its utilization as a decorative coating in construction material helps protect from sunlight and pollution, while its incorporation in pavement materials enables the decomposition of vehicle-induced gases ([Chen et al., 2012](#); [Shchelokova et al., 2021](#)).

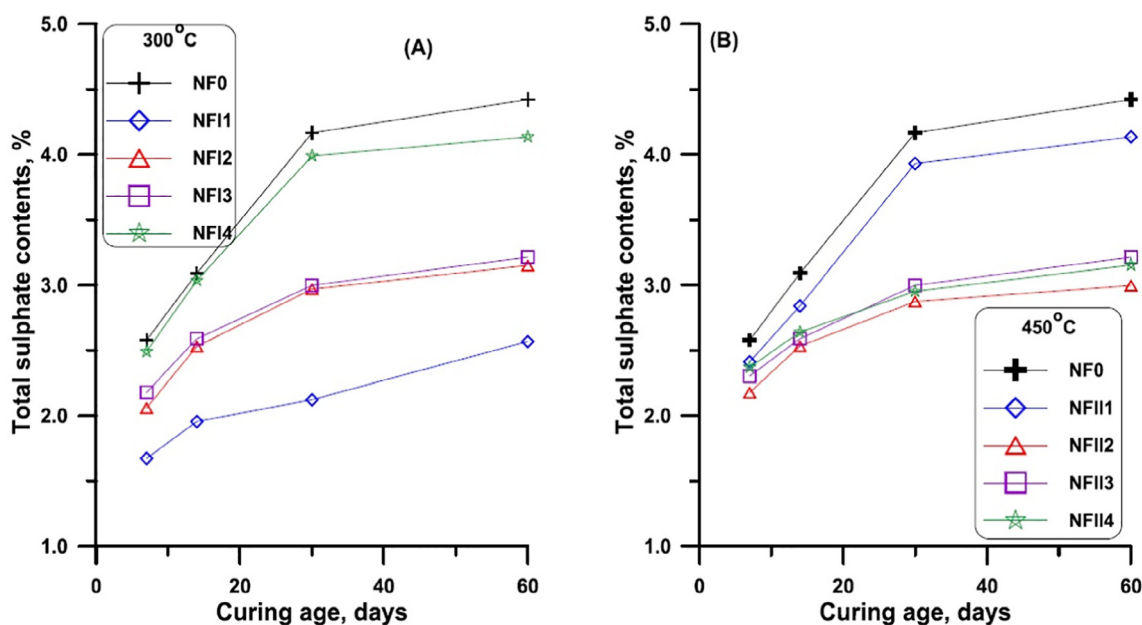


Fig. 11. Compressive strength of a sulfate-attacked NF specimen, where NF0 is the control, NF (1–4) contains respectively 0.5%, 1%, 1.5%, and 2% NF ([Heikal et al., 2021](#)).

The photocatalytic property of nano-TiO₂ can help decompose gaseous pollutants, enhancing and optimizing the performance of concrete (Meng et al., 2012). The X-ray diffraction (XRD) of NT exhibits a smooth hump confirming the amorphous phase, suitable for use in cementitious matrices (Fig. 12). The peaks labeled ‘R’ and ‘A’ denote rutile and anatase phases (Daniyal et al., 2019). The first available research on nano-TiO₂ (NT) concrete was carried out by Li et al. (2006) from the Harbin Institute of Technology, China. The abrasion resistance of concrete that included 1% nano-TiO₂ provided better results than polypropylene and nano-silica. The concrete mixtures incorporating 5% NT exhibited super-hydrophilicity at almost zero water contact angle after 2 h of direct sunlight exposure, and the surface reflectance recovered after 1 h of direct sunlight exposure (Sanalkumar and Yang, 2021).

NT particles exhibit no pozzolanic reactions, acting as non-reactive fine fillers to refine pore structures. NT can accelerate cement hydration, providing additional nucleation sites and increasing water demand with reduced setting time. The main peak heat of hydration occurs early with enhanced intensity, while the duration of occurrence decreases compared to the control specimen (Chen et al., 2012). It was observed by Xu et al. (2020) that for recycled aggregate (RA) concrete at 0.35 w/b and an aggregate to binder ratio of 3, when 50% of the virgin aggregate is replaced by RA, the addition of 5% fly ash and 0.3 optimal quantity of NT, the harmful pollutant nitrogen oxide (NO_x) was degraded by 70%, indicating a highly durable photocatalytic performance. The utilization of NT in recycled aggregate con-

crete can reduce the quantity of carbon dioxide, as mentioned in Fig. 13 by Moro et al. (2020). Karthikeyan and Dhinakaran (2018) discussed that the optimum quantity of NT was 0.5 wt% with 9.5% silica fumes and 0.5 vol% steel fibers.

3.4.1. Effect of Nano- TiO₂ on the properties of concrete

Joshaghani et al. (2020) and Jalal et al. (2013) reported that the high surface area of NT and its tendency to absorb more water caused a reduction in slump flow. Acceptable workability was observed at 3% NT while incorporating 5% NT drastically reduced workability (and showed more viscous behavior, which further affected the rheological properties of the self-compacting concrete). The concrete was filled in the molds without any induced vibrations, and the presence of NT improved the consistency, reducing the segregation and bleeding of concrete. The fluidity of the cement mortar decreased by 21% and 40% with the inclusion of 5% and 10% NT, respectively, significantly improving with the addition of superplasticizer and slag (Meng et al., 2012).

The microstructural properties of NT concrete were studied by Feng et al. (2013), who identified three types of nano-modification mechanisms caused by NT in a cementitious matrix. First, NT acted as activator nuclei by producing needle-shaped hydration products that fill the micro-pores. Second, the emergence of a homogeneous dense calcium-silicate-hydrate (CSH) gel was facilitated. Third, the NT particles aided in the sustained disposition of hydration products throughout the cement matrix. It was demonstrated by Ren et al. (2018) that the NT

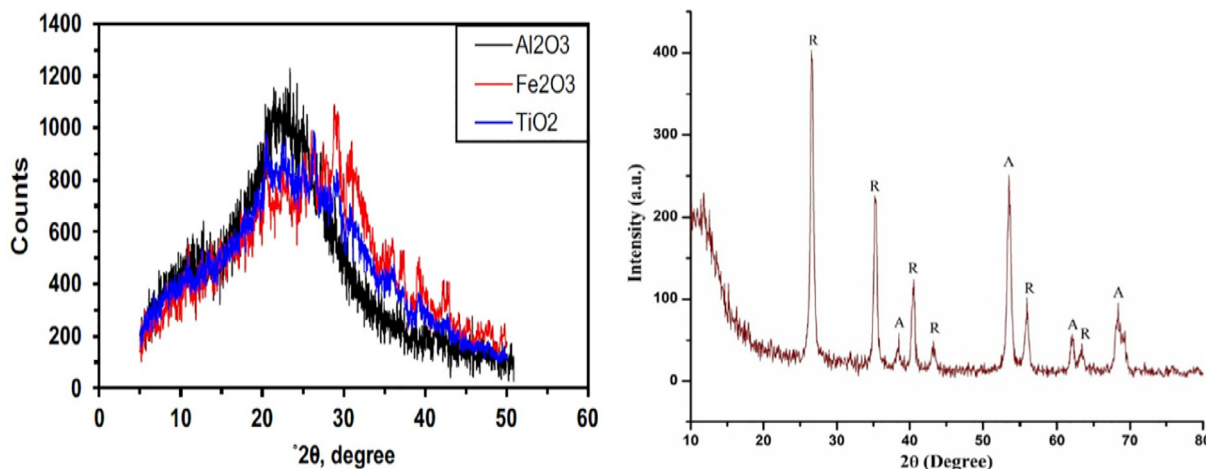


Fig. 12. XRD patterns for nano-Al₂O₃, nano-Fe₂O₃, and nano-TiO₂ (Joshaghani et al., 2020; Daniyal et al., 2019).

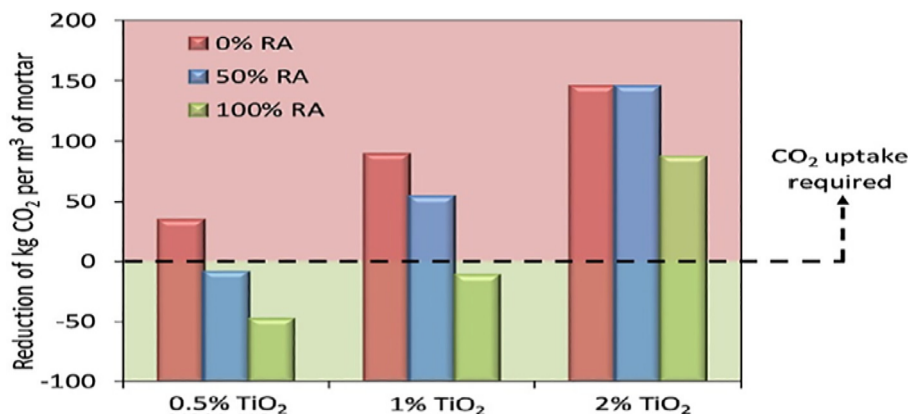


Fig. 13. Variation in CO₂ reduction with TiO₂ content in concrete containing recycled aggregates (RA) (Moro et al., 2020).

particles could act as fillers and as crystallization centers of calcium hydroxide, which can trim the crystal sizes at the paste-aggregate interface, improving the structure and material properties. The NT can consume calcium hydroxide in the cement paste and generate calcium titanate, which can be detrimental for the concrete at later ages.

The introduction of NT improved the pore structure, acting as a filler and enhancing concrete density. It activates the cement hydration and also reduces the size of calcium hydroxide crystals. When the quantity of NT was more than 4%, the crystal quantity of $\text{Ca}(\text{OH})_2$ was reduced because of the limited growing space. This increases shrinkage and creep, leading to a looser cement matrix pore structure and subsequent reduction in the desired concrete properties (Jalal et al., 2013).

It was observed by Meng et al. (2012) that the addition of 5% and 10% NT improved the 1-day strength by 46% and 47%, respectively, while it reduced the 28-day strength by 6% and 9%, respectively, compared with the control specimen. The addition of superplasticizer and slag powder with the NT improved the 28-day compressive strength by 15% and 7%, respectively. Nikbin et al. (2019) noted 40% more strength (48.4 MPa compared to 34 MPa for the control) with the addition of 6 wt% NT. The ultrasonic pulse velocities (UPVs) for concrete containing 6% and 8% NT were in the excellent ranges of 4.65 and 4.52 km/s, respectively. The addition of 3% NT improved the compressive strength by 19.2% (Chinthakunta et al., 2021). It was identified by Sun et al. (2020) that cement paste that included 5 nm particles exhibited better compressive strength when compared with 25 nm size. The optimal value was obtained for 5 nm size NT at 0.5 wt% with 0.3 water to cement ratio. This mixture exhibited an 18.7% increment in the compressive strength at 7 days and 24.35% at 28 days.

Jalal et al. (2013) noted that the flexural strength improved when adding up to 4 wt% but decreased beyond that. Meng et al. (2021) demonstrated the ball-milling method to disperse NT on the surface of fly ash, used as a supplementary cementitious material (SCM). At 1 wt% NT (with a 30-minute ball-milling duration), a dramatic enhancement of 37.74% in flexural strength was obtained. Sastry et al. (2020) recorded enhancements of 32.63% in flexural strength and 22.22% in split tensile strength at 5% NT. The impact resistance of concrete that included NT was studied by Nikbin et al. (2019). It was noted that a specimen that incorporated 6% NT had 66% more impact resistance when compared with the control blend. The number of blows taken by the control specimen until first crack and ultimate failure was 11 and 15, respectively, compared to 18 and 25 for a 6 wt% NT specimen. After first cracking, the NT specimen resisted 36% more strikes until ultimate failure.

The water absorption properties of the NT concrete were investigated by Jalal et al. (2013), who noted that the capillary absorption height and the percentage of water absorption declined for NT content up to 4% because of the high reactivity and filler effect of the NT particles. The water absorption for the control and 4 wt% NT concrete at 168 h of exposure were 5.12% and 4.22%, respectively. When the substitution was above 4%, the water absorption increased because of the unsuitable dispersion and agglomeration in the cement paste. The high surface area of the nanoparticles promotes hydration and reduces the porosity, which subsequently reduces the depth of water penetration. The effect of NT was inferior when compared with nano-alumina and nano-iron oxide (Joshaghani et al., 2020).

Jalal et al. (2013) noted a gradual reduction in the chloride penetration depth with increasing amounts of NT particles. The chloride penetration was 0.13% and 0.09% with 3% and 4% NT, respectively, while the control concrete was 0.23%. The rapid chloride penetration and chloride migration were gradually reduced with the addition of NT (Joshaghani et al., 2020). The rapid chloride penetration charges passed through concrete containing fly ash, silica fume, and NT was 115.5 C compared with 970.83 C for the control concrete (Chinthakunta et al., 2021).

The electrical resistivity of concrete containing fly ash, silica fume, and NT was very high (142.20 k Ω -cm), as observed by Chinthakunta et al. (2021), showing a negligible corrosion rate at 90 days compared with the 19.8 k Ω -cm of the control mixture. Daniyal et al. (2019) noted a significantly lower corrosion rate in the NT specimens at all exposure conditions, while the best results were observed at 3% NT. Mohseni et al. (2018) noted electrical resistivities of control specimens between 5 and 10 k Ω -cm (high probability of corrosion), while those of concrete containing 10%–15% rice husk ash (RHA) and 3%–5% NT are above 20 k Ω -cm, indicating a very low corrosion probability. Rao et al. (2015) studied the resistance to carbonation, noting that specimens incorporating 0.5 wt%, 0.75 wt%, and 1 wt% NT were practically impermeable to carbonation after 91 days of exposure. Duan et al. (2016) noted an improved resistance to carbonation by 77%, 62%, and 42% for specimens containing 1%, 3%, and 5% NT, respectively, after 180 days of exposure.

Zhang et al. (2015) reported that the drying shrinkage of a blend incorporating 25 nm NT at 5 wt% was mitigated because of reduced water loss by the pore filling effect. The shrinkage of control mortars was higher in the first 6 days, sharply increasing on days 5–15 of hydration. Similar studies by Duan et al. (2016) noted reduced shrinkage after 5 days for a 1% NT specimen and 2 days for 2% and 5% NT specimens compared with a control specimen. Sastry et al. (2020)

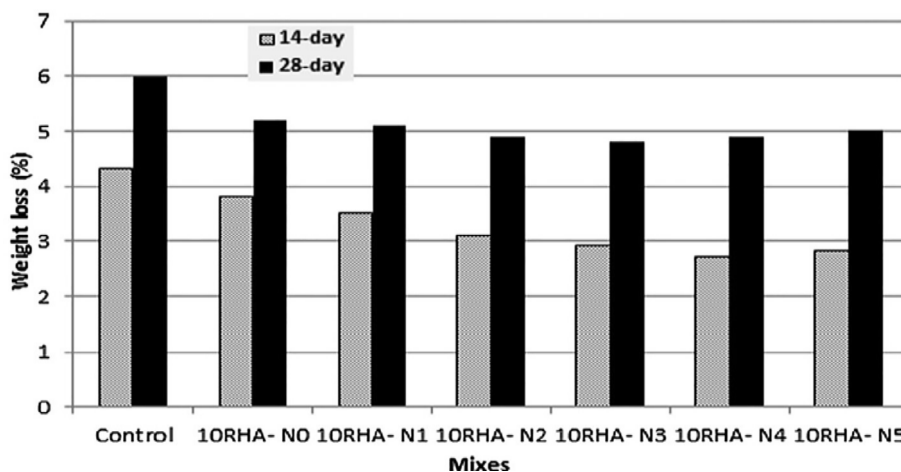


Fig. 14. Weight loss of Portland cement concrete with RHA subjected to hydrochloric acid attack. RHA is rice husk ash, N is NT. (Praveenkumar et al., 2019).

examined the resistance of control and NT specimens to a 5% magnesium sulfate solution. The control specimen had a weight loss of 4.383%, while the weight losses were 2.079%, 1.708%, and 1.09%, respectively, for specimens incorporating 3%, 4%, and 5% NT. Similarly, the control specimen had a 1.44% loss in compressive strength after 28 days, while concrete incorporating 3%, 4%, and 5% NT had losses of 1.02%, 0.896%, and 0.80%, respectively.

The resistance of NT specimens to hydrochloric acid attack was analyzed by Praveenkumar et al. (2020), as shown in Fig. 14. More significant weight loss was observed at 28 days than at 14 days. The concrete blended with 10% RHA and 3% NT offered the highest resistance to hydrochloric acid attack. Daniyal et al. (2019) noted high resistance for NT concrete specimens under acid attack. After 360 days of exposure to acid, the compressive strength of the control and 1%, 3%, and 5% NT were 34.5, 40.3, 42.7, and 43.4 MPa, respectively. It was correspondingly 27.37%, 22.94%, 21.51%, and 21.38% less when compared with specimens immersed in tap water for 360 days.

Farzadnia et al. (2013) noted that the NT concrete exhibited higher residual compressive strength, brittleness, and gas permeability than a control specimen for temperatures up to 600 °C. NT lowered the mass loss to 300 °C, while it increased from 300 to 100 °C. After exposure to 110–650 °C temperatures, the average weight loss for control concrete was 13.5%, while for concrete including 3% and 4% NT, the mass losses were 16.7% and 17.5%, respectively. Nikbin et al. (2020) observed a minimum compressive strength loss of 15.5 at 600 °C for a specimen incorporating 2% NT, and the highest weight loss (6.9%) was observed for 6% NT samples. Increasing the quantity of NT gradually increased the losses in compressive strength and weight.

4. Combinations of various nanomaterials

Various researchers have investigated the characteristics of concrete incorporating two or more nanomaterials. The properties of TiO₂-graphene composites with 0.01 wt%, 0.03 wt%, and 0.05 wt% were studied by Zhang et al. (2021). A crumpled morphology with 20–30 nm particle sizes was observed with transmission electron microscopy. The dosage level of 0.03 wt% promoted the formation of C-A-S-H phases, providing nucleation sites for the development of hydration phases. There was a 26.6% increase in compressive strength and an 11.3% increase in flexural strength compared to the control concrete. The capillary sorptivity coefficient decreased from 0.635 to 0.432 mm/min^{0.5}, and a 68.7% reduction in chloride penetration with the optimal quantity of 0.03 wt% was observed. It was noted by Guo et al. (2021) that the addition of 0.5% TiO₂-Graphene to the epoxy resin polymer matrix reduced the capillary sorptivity by 52.22% and the chloride diffusion coefficient by 77.43%.

The combined effect of NS, NT, and NC was investigated by Ren et al. (2021). The compressive strengths of a mixture incorporating 2 wt% NT, 2 wt% NC, and 0.5 wt% NS at 1, 3, and 7 days were respectively 52.54%, 53.76%, 61.09% higher than the control specimens. This combined addition can improve the rate of hydration and produce more calcium hydroxide, reducing the total porosity from 23.2% to 16.8%. The optimum dosages for NS, NT, and NC have been identified analytically (using the response surface methodology) as 0.86 wt%, 2.75 wt%, and 0.14 wt%, respectively, producing 83 MPa compressive strength at 7 days.

The individual characteristics of TiO₂ (self-cleansing and bactericidal) and SiO₂ (significant mechanical properties) were combined by various researchers to produce nanocomposite concrete blends. The negative charges on the TiO₂-SiO₂ nanocomposite surface can uniformly distribute in the concrete blend. The compressive strength, flexural strength, and dynamic compressive strength improved (Han et al., 2019). The nanocomposite improves the rate of hydration and reduces the porosity compared with the individual use of TiO₂ (Sun et al., 2017). Incorporating 3 wt% of TiO₂-SiO₂ nanocomposite improved

the compressive strength because of increased C-S-H and a compact microstructure (Sikora et al., 2017). The use of 3% TiO₂-SiO₂ improves the compressive strength of the reactive powder concrete by 12.26%, while 5% improves the flexural strength by 87% (Han et al., 2017). It was noted by Shchelokova et al. (2021) that the optimal quantity of the TiO₂-SiO₂ nanocomposite calcined at 800 °C is 0.1 wt% to 0.5 wt%. It exhibited peak photocatalytic activity, better mechanical properties, and reduced porosity, water absorption, and abrasion losses.

5. Discussion

Nanoclay is a nanofiller with an average particle size roughly 1000 times finer than cement grains. Calcination at an optimal temperature of 750 °C plays a vital role in enhancing the pozzolanic reactivity of nanoclay. The pore structure of cement paste becomes refined because of the pozzolanic, nucleation, and filler effect. It improves the mechanical properties, electrical resistivity, toughness, and elastic modulus of the cement blend, reducing water, acid, and chloride penetration. Shrinkage in nanoclay concrete may vary with the different types of nanoclay because their morphology and chemical compositions may notably influence it. After exposure to high temperatures, the compressive strength, tensile strength, and flexural strength is improved for the nanoclay concrete compared with control specimens.

Nano-CaCO₃ can accelerate the hydration of cementitious materials because of nucleation effects and filler characteristics. Its incorporation can gradually reduce the workability and initial and final settings with increasing nano-CaCO₃ content. It can enhance the compressive, flexural, splitting, and bond strength while reducing water sorptivity, chloride penetration, and acid attack. The shrinkage and behavior at high temperatures need further investigation, as researchers have reported contradicting results.

The addition of nano-Fe₂O₃ refines the pore structure and increases the viscosity of the cement matrix, significantly reducing microcracks and providing a compact microstructure. Compared to the other nanomaterials, the incorporation of NF improved the workability of concrete. It also improved the mechanical properties and electrical resistivity, reducing water absorption, chloride penetration, and sulfate attack. The behavior at high temperatures needs further studies due to non-conclusive results. Also, a research gap is observed concerning shrinkage, acid attack, and corrosion of concrete specimens.

The use of nano-TiO₂ has been researched intensely. Nano-TiO₂ concrete fills molds without any induced vibrations, improving consistency and reducing the segregation and bleeding of concrete. NT can consume calcium hydroxide in the cement paste and generate calcium titanate, which can be detrimental to the concrete at later ages. NT improves mechanical properties, electrical resistivity, and impact resistance, reducing shrinkage, water absorption, acid, sulfate, and chloride ingress. NT concrete exhibited higher residual compressive strength, brittleness, and gas permeability than the control specimen for temperatures up to 600 °C.

6. Comparison of property enhancements among nanomaterial additives

Incorporating nano-TiO₂, nano-Fe₂O₃, nano-clay/metakaolin, and nano-CaCO₃ to partially replace cement/geopolymer paste or as an additive in cementitious matrices has significant potential for application in civil engineering. When properties are compared (as in Fig. 15 and Tables 2–4), it was noted that the workability was gradually reduced with nanomaterial incorporation, which could be overcome using a proper superplasticizer. Concrete incorporating nano-CaCO₃ exhibited better mechanical properties in terms of compressive strength, flexural strength, and split tensile strength. It also offered high electrical resistivity, water absorption resistance, elevated tem-

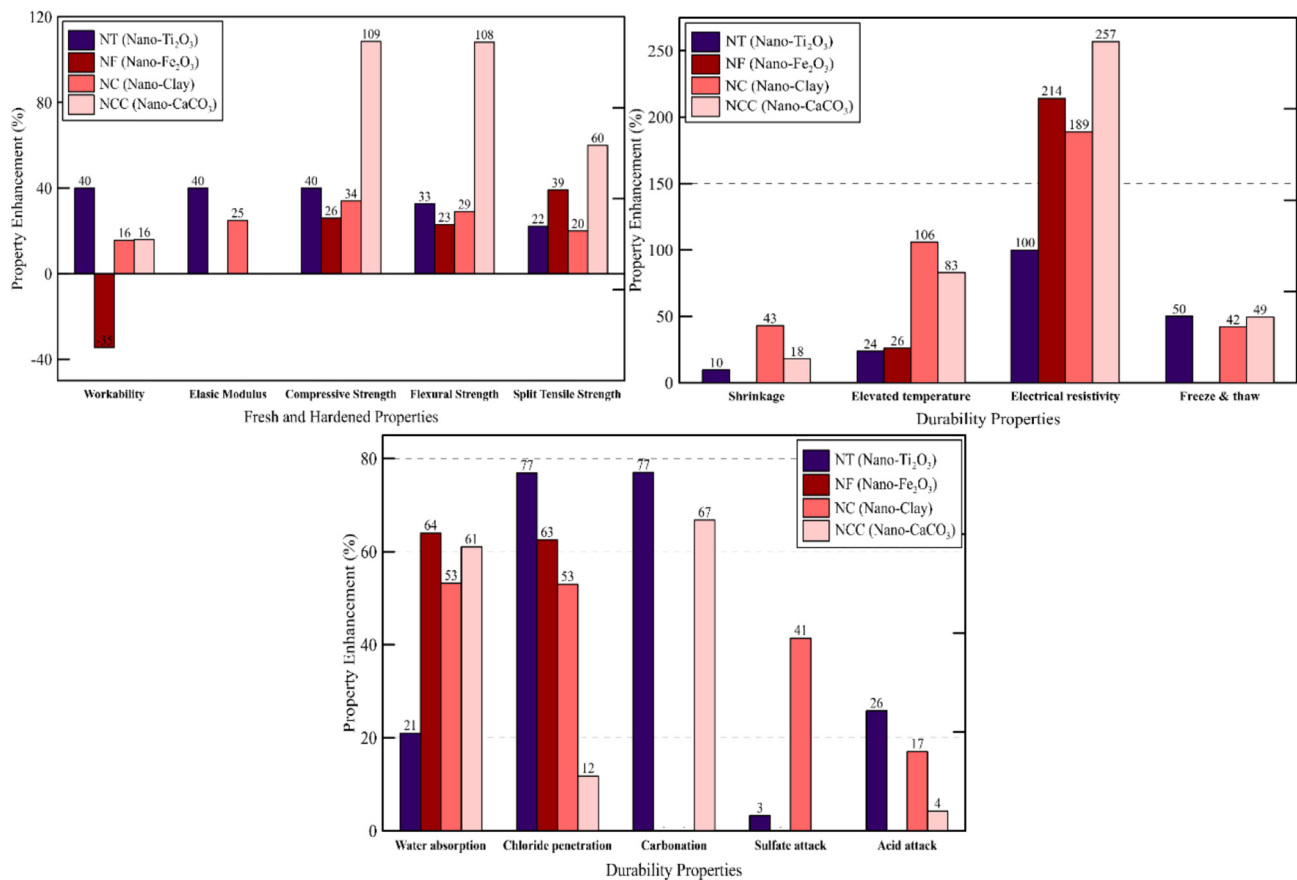


Fig. 15. Comparison of fresh, transport, mechanical, and durability properties of concrete containing various nanomaterials.

perature behavior, and freeze–thaw durability, while the resistance to chloride penetration was minimal compared with other nanomaterials.

TiO₂ offered the highest elastic modulus, workability, and resistance against chloride penetration, carbonation, acid attack, and freeze–thaw damage. The mechanical properties were also enhanced with the utilization of nano-TiO₂. It was also noted that nano-Fe₂O₃ negatively affected concrete workability while offering high resistance to water absorption and chloride penetration, and high electrical resistivity.

To the best of the authors’ knowledge, a research gap was noted for the elastic modulus, carbonation effect, sulfate attack, acid attack, freeze–thaw durability, and shrinkage. Superior resistance at elevated temperatures was observed for concrete mixes incorporating nanoclay. The combination of various nanomaterials in binary or ternary form can be investigated to produce superior quality concrete having high mechanical and durability properties. Based on the literature, the optimal replacement levels of nano-TiO₂ (1 wt%–4 wt%), nano-Fe₂O₃ (1 wt%–3 wt%), nano-clay (5 wt%–7.5 wt%), nano-metakaolin (0.5 wt%–2 wt%), and nano-CaCO₃ (0.5 wt%–2 wt%) are recommended.

7. Conclusions

This paper presents a comprehensive review and findings on earlier research studies and current trends in concrete containing nanomaterials, including nano-TiO₂, nano-Fe₂O₃, nano-clay/metakaolin, and nano-CaCO₃. The influence of these nanomaterials on the fresh properties, microstructure, mechanical, and durability characteristics of cement/geopolymer concrete were analyzed. Based on the analysis of various studies following conclusions are drawn:

- Nanoclays are crystalline layers of mineral silicates possessing pozzolanic properties. They provide rich sources of aluminosilicates that react with calcium hydroxide to form C-S-H and C-A-H gels, leading to improvements in the mechanical and durability properties of cementitious composites. Incorporating nanoclay up to 2 wt % reduces porosity and develops a dense matrix microstructure. However, higher nanoclay content adversely affects workability and mechanical strength. Nano-metakaolin up to 6 wt% and a quantity (0.02%) of carbon nanotubes improve nanoparticle dispersion and mechanical properties. The inclusion of nano-metakaolin also reduces the permeability of the matrix, which was indicated by the reduced chloride ion penetration results.
- Nano-CaCO₃ can be used as a filler to densify the microstructure of the cementitious matrix. The properties of cement mortar and concrete, such as workability, setting times, and mechanical strengths, can be significantly improved with the addition of nano-CaCO₃ by up to 3%. Nano-Fe₂O₃ (NF) addition accelerates the formation of C-S-H gel due to its better dispersion and nano-filling effects. Nano-Fe₂O₃ generates nano-reinforcing material when reacting with the calcium hydroxide in the matrix, resulting in the densification of the concrete microstructure. NF also helps in accelerating cement hydration. Nano-TiO₂ (NT) acts as a non-reactive nano-filler and plugs the pores, leading to refinement of the pore structure. However, the higher surface area of NT particles reduced the workability of the mix. NT blended with other SCMs significantly enhances cement concrete’s mechanical strength and durability properties.
- The findings have confirmed the optimal dosage of these nanomaterials and the possibility of using combinations of various micro and nanomaterials to attain superior properties. Concrete containing a combination of various nanomaterials in appropriate propor-

Table 2
Fresh and mechanical properties of Nanomaterials.

Properties→ Nanomaterials↓	Workability	Density, Elastic modulus	Compressive strength	Flexural strength	Splitting tensile
Nano-TiO ₂	The workability reduced by 40% with 1.5 wt% (Sorathiya et al., 2017)	40% enhancement with 6% Nt when compared with 4% NT. (Ng et al., 2020)	40% more strength with the addition of 6 wt% NT (Nikbin et al., 2019)	Enhancement by 32.63% in the flexural strength at 5% NT. (Sastry et al., 2020)	Enhancement by 22.22% in split tensile strength at 5% NT. (Sastry et al., 2020)
Nano-Fe ₂ O ₃	34.5% increase in the slump flow with the incorporation of 2% NF (Feng et al., 2020)	- Research gap	Improved by 26% and 14.5% for the addition of 3 and 5% NF respectively, (Li et al., 2004, 2004a)	Improved by 17.8% and 23% respectively for 3 and 5% NF respectively, (Li et al., 2004, 2004a)	39.13% improvement with 1% NC (Nazari and Riahi, 2011)
Nano-clay	9% nano-metakaolin reduced the concrete slump by 15.7% (Norhasri et al., 2016).	25% enhancement with 3% calcined clay. (Alharbi et al., 2021)	34% increase with 7.5% nano-clay (Morsy et al., 2014)	29% increase with 7.5% nano-clay (Morsy et al., 2014)	20% increase with 7.5% nano-clay Hamed et al., (2019),
Nano-CaCO ₃	16% reduction in the slump with 2% Nano-CaCO ₃ (Shaikh and Supit, 2014).	- Research gap	108.6% improvement with 2 wt% (Liu et al., 2012)	108.3% improvement with 1 wt% (Liu et al., 2012)	60% higher splitting tensile strength with 3% Nano-CaCO ₃ (Su et al., 2016)

Table 3
Transport properties of nanomaterials.

Properties→ Nanomaterials↓	Water absorption	Chloride penetration	Carbonation	Sulfate attack	Acid attack
Nano-TiO ₂	21% reduction with 4% NT (Jalal et al., 2013)	76.9% improvement with 3% NT (Jalal et al., 2013)	Improved resistance to carbonation by 77%, 62% and 42% for 1,3 and 5% NT (Duan et al., 2016)	Weight loss got improved by 3.29%, compressive strength loss improved by 0.64% (Sastry et al., 2020)	25.79% improvement in the compressive strength at 5% NT (Daniyal et al., 2019)
Nano-Fe ₂ O ₃	64% reduction with 5% NF (Joshaghani et al., 2020).	About 62.5% improvement in the chloride migration coefficient. (Joshaghani et al., 2020)	- Research gap	The compressive strength of specimens containing 0.5 and 1% NF (processed at 300 °C) was higher than that of the control concrete (Heikal et al., 2021),	- Research gap
Nano-clay	53.2% reduction with 3% nano-clay. (Langaroudi et al., 2018)	53% reduction in chloride penetration with 5% NC Fan and Zhang (2014)	- Research gap	41.4% reduction with 9% nano metakaolin (Diab et al., 2019)	17% reduction in compressive strength loss with 3% nano-clay. (Fan et al., 2016)
Nano-CaCO ₃	The capillary water absorption of the concrete containing 2% NC was reduced by 61% (Khotbehsara et al., 2018).	The chloride permeability at 28 and 90 days reduced by 11.8 and 7.7% (Shaikh and Supit, 2015)	66.8% improvement in the carbonation with 3% NC (Li et al., 2020)	- Research gap	4.2% reduction with 1% Nano-CaCO ₃ (Bankir et al., 2020),

Table 4
Other durability properties of nanomaterials.

Properties→ Nanomaterials↓	Shrinkage	Microstructure	Elevated temperature	Electrical resistivity	Freeze and thaw
Nano-TiO ₂	9.6% lower shrinkage was noted in the 1% NT concrete (Chunping et al., 2018)	NT particles fill the empty space and as crystallization centers of calcium hydroxide, improving the structure and the material properties. (Ren et al., 2018)	23.70% enhanced weight loss at 110–650 °C for 3% NT (Farzadnia et al., 2013)	100% enhancement with 2% NT (Mohseni et al., 2018)	About 50% reduction in the mass loss of 1% NT concrete after 800 freeze–thaw cycles (Chunping et al., 2018)
Nano-Fe ₂ O ₃	- Research gap	The addition of NF refines the pore structure and increases the viscosity of the cement matrix. (Khoshakhlagh et al., 2012).	The compressive strength reduction was 24 and 26% less for the concrete containing 2 and 3% NF at 600 °C. (Abo-El-Enein et al., 2018)	214.3% enhancement with 2% NF Madandoust et al., (2015)	-Research gap
Nano-clay	The autogenous shrinkage of mortar incorporating 1.3 and 3% of nano clay reduced respectively 43 and 40% (Polat et al., 2015)	The pore structure of cement paste got refined on account of the pozzolanic and filler effect of the nano clay (Fan et al., 2016).	At 600 °C, the compressive strength, tensile strength, and flexural strength was enhanced by 15%, 27%, and 106% with 2% NC (Irshidat and Al-Saleh, 2018).	189% enhancement with 3% nano-clay. (Alharbi et al., 2021)	14.68% reduced mass loss, 42% reduced compressive strength loss at 3% nano clay (Langaroudi and Mohammadi, 2018)
Nano-CaCO ₃	18% reduced shrinkage for the specimens containing 5% NC (Camiletti et al., 2013)	The porosity of the control specimen was 15.2% which reduced to 12% with 3.2% of NC content. (Wu et al., 2018a)	83% reduction in the sum of weight loss of cement at 600–800 °C when 1% NC (Salih et al., 2020)	257% improvement with 4% NC (Khotbehsara et al., 2018)	49.48% reduction with 1–3% of NC (Sun et al., 2020a)

tions can eliminate most of the drawbacks. The main barrier to the successful utilization of nanomaterials is dispersion, which various researchers successfully overcame. The comparison chart clarifies the overall work done and opens the door for further studies to fill the research gaps. More focused research needs to be conducted in this area, which seems to be a promising and vital contribution towards construction industry sustainability.

Acknowledgments

Support for the research presented in this paper was provided by Riad Sadek, Endowed Chair in Civil Engineering of the American University of Sharjah, and is gratefully acknowledged. The views and conclusions in this study, whether expressed or implied, are those of the authors and should not be interpreted as those of the supporting institution.

References

- Abo-El-Enain, S.A., El-Hosiny, F.I., El-Gamal, S.M., Amin, M.S., Ramadan, D.M., 2018. Gamma radiation shielding, fire resistance, and physicochemical characteristics of Portland cement paste modified with synthesized Fe₂O₃ and ZnO nanoparticles. *Constr. Build. Mater.* 10 (173), 687–706.
- Abo-El-Enain, S.A., Amin, M.S., El-Hosiny, F.I., Hanafi, S., ElSokkary, T.M., Hazem, M.M., 2014. Pozzolanic and hydraulic activity of nano-metakaolin. *HBRC J.* 10 (1), 64–72.
- Al-Khafaji, M.K., Abbas, W.A., Al-Mishhadani, S., 2016. Behavior of High Strength Concrete Containing Nano-Metakaolin Exposure to Fire Flame. *Eng. Technol. J.* 34, 857–875.
- Alharbi, Y.R., Abadel, A.A., Mayhoub, O.A., Kohail, M., 2021. Effect of using available metakaolin and nano materials on the behavior of reactive powder concrete. *Constr. Build. Mater.* 1, (269) 121344.
- Allalou, S., Kheribet, R., Benmounah, A., 2019. Effects of calcined halloysite nano-clay on the mechanical properties and microstructure of low-clinker cement mortar. *Case Stud. Constr. Mater.* 1, (10) e00213.
- Amin, M.S., El-Gamal, S.M., Hashem, F.S., 2013. Effect of addition of nano-magnetite on the hydration characteristics of hardened Portland cement and high slag cement pastes. *J. Therm. Anal. Calorim.* 112 (3), 1253–1259.
- Andrew, R.M., 2018. Global CO₂ emissions from cement production. *Earth Syst. Sci. Data* 10 (1), 195–217.
- Assaedi, H., Alomayri, T., Kaze, C.R., Jindal, B.B., Subaer, S., Shaikh, F., Alraddadi, S., 2020. Characterization and properties of geopolymer nanocomposites with different contents of nano-CaCO₃. *Constr. Build. Mater.* 20, (252) 119137.
- Bankir, M.B., Ozturk, M., Sevim, U.K., Depci, T., 2020. Effect of n-CaCO₃ on fresh, hardened properties and acid resistance of granulated blast furnace slag added mortar. *J. Build. Eng.* 1, (29) 101209.
- Bergaya, F.B., Lagaly, G. General introduction: clays, clay minerals, and clay science. *Developments in clay science 2013 Jan 1* (Vol. 5, pp. 1-19). Elsevier.
- Batuecas, E., Liendo, F., Tommasi, T., Bensaid, S., Deorsola, F.A., Fino, D., 2021. Recycling CO₂ from flue gas for CaCO₃ nanoparticles production as cement filler: A Life Cycle Assessment. *J. CO₂ Util.* 1, (45) 101446.
- Braganca, M.O., Portella, K.F., Bonato, M.M., Alberti, E., Marino, C.E., 2016. Performance of Portland cement concretes with 1% nano-Fe₃O₄ addition: Electrochemical stability under chloride and sulfate environments. *Constr. Build. Mater.* 1 (117), 152–162.
- Camiletti, J., Soliman, A.M., Nehdi, M.L., 2013. Effects of nano-and micro-limestone addition on early-age properties of ultra-high-performance concrete. *Mater. Struct.* 46 (6), 881–898.
- Chen, J., Kou, S.C., Poon, C.S. Hydration and properties of nano-TiO₂ blended cement composites. *Cement and Concrete Composites.* 2012 May 1;34(5):642-9.
- Chinthakunta, R., Ravella, D.P., Sri Rama Chand, M., Janardhan Yadav, M., 2021. Performance evaluation of self-compacting concrete containing fly ash, silica fume and nano titanium oxide. *Mater. Today: Proc.* 43, 2348–2354.
- Chunping, G., Qiannan, W., Jintao, L., Wei, S., 2018. The effect of nano TiO₂ on the durability of ultra-high-performance concrete with and without a flexural load. *Ceram-Silikaty.* 1 (62), 374–381.
- Cosentino, I., Liendo, F., Arduino, M., Restuccia, L., Bensaid, S., Deorsola, F., Ferro, G.A., 2020. Nano CaCO₃ particles in cement mortars towards developing a circular economy in the cement industry. *Procedia Struct. Integrity* 1 (26), 155–165.
- Daniyal, M., Akhtar, S., Azam, A., 2019. Effect of nano-TiO₂ on the properties of cementitious composites under different exposure environments. *J. Mater. Res. Technol.* 8 (6), 6158–6172.
- Duan, P., Yan, C., Luo, W., Zhou, W., 2016. Effects of adding nano-TiO₂ on compressive strength, drying shrinkage, carbonation and microstructure of fluidized bed fly ash based geopolymer paste. *Constr. Build. Mater.* 1 (106), 115–125.
- Diab, A.M., Elyamany, H.E., Abd Elmoaty, M., Sreh, M.M., 2019. Effect of nanomaterials additives on performance of concrete resistance against magnesium sulfate and acids. *Constr. Build. Mater.* 20 (210), 210–231.
- Ding, Y., Liu, J.P., Bai, Y.L., 2020. Linkage of multi-scale performances of nano-CaCO₃ modified ultra-high performance engineered cementitious composites (UHP-ECC). *Constr. Build. Mater.* 20, (234) 117418.
- Fan, Y., Zhang, S., Kawashima, S., Shah, S.P., 2014. Influence of kaolinite clay on the chloride diffusion property of cement-based materials. *Cem. Concr. Compos.* 1 (45), 117–124.
- Fan, Y., Zhang, S., Wang, Q., Shah, S.P., 2015. Effects of nano-kaolinite clay on the freeze-thaw resistance of concrete. *Cem. Concr. Compos.* 1 (62), 1–2.
- Fan, Y., Zhang, S., Wang, Q., Shah, S.P., 2016. The effects of nano-calcined kaolinite clay on cement mortar exposed to acid deposits. *Constr. Build. Mater.* 15 (102), 486–495.
- Fan, Y.F., Zhang, F., 2014. Mechanical and chloride diffusion behavior of kaolinite clay modified cement-based material. *J. Civ. Architect. Environ. Eng.* 36 (1), 130–137.
- Farzadnia, N., Ali, A.A., Demirboga, R., Anwar, M.P., 2013. Characterization of high strength mortars with nano Titania at elevated temperatures. *Constr. Build. Mater.* 1 (43), 469–479.
- Farzadnia, N., Ali, A.A., Demirboga, R., Anwar, M.P., 2013a. Effect of halloysite nanoclay on mechanical properties, thermal behavior and microstructure of cement mortars. *Cem. Concr. Res.* 1 (48), 97–104.
- Feng, D., Xie, N., Gong, C., Leng, Z., Xiao, H., Li, H., Shi, X., 2013. Portland cement paste modified by TiO₂ nanoparticles: a microstructure perspective. *Ind. Eng. Chem. Res.* 52 (33), 11575–11582.
- Ghazanlou, S.I., Jalaly, M., Sadeghzadeh, S., Korayem, A.H., 2020. A comparative study on the mechanical, physical and morphological properties of cement-micro/nano Fe₃O₄ composite. *Sci. Rep.* 10 (1), 1–4.
- Giannelis, E.P., Krishnamoorti, R., Manias, E., 1999. Polymer-silicate nanocomposites: model systems for confined polymers and polymer brushes. *J. Eng. Sci.* 107–147.
- Ghazy, M.F., Elaty, M.A., Elkhoriy RS. Performance of blended cement mortars incorporating nano-metakaolin particles at elevated temperatures. *Proceeding of the International Conference on Advances in Structural and Geotechnical Engineering, Hurghada, Egypt 2015 Apr* (pp. 6-9).
- Ghodke, S., Bhanvase, B., Sonawane, S., Mishra, S., Joshi, K. Nanoencapsulation and nanocontainer based delivery systems for drugs, flavors, and aromas. *Encapsulations 2016 Jan 1* (pp. 673-715). Academic Press.
- Guo, S.Y., Luo, H.H., Tan, Z., Chen, J.Z., Zhang, L., Ren, J., 2021. Impermeability and interfacial bonding strength of TiO₂-graphene modified epoxy resin coated OPC concrete. *Prog. Org. Coat.* 1, (151) 106029.
- Guo, X., Yang, K., Fan, Y., 2018. Study on reasonable addition of nano metakaolin in cement mortar in chloride environment. *Concrete.* 5, 110–114.
- Guggenheim, S., Martin, R.T., 1995. Definition of clay and clay mineral: joint report of the AIPEA nomenclature and CMS nomenclature committees. *Clays Clay Miner.* 43 (2), 255–256.
- Hakamy, A., Shaikh, F.U., Low, I.M., 2015. Effect of calcined nanoclay on microstructural and mechanical properties of chemically treated hemp fabric-reinforced cement nanocomposites. *Constr. Build. Mater.* 1 (95), 882–891.
- Hakamy, A., Shaikh, F.U., Low, I.M., 2015a. Characteristics of nanoclay and calcined nanoclay-cement nanocomposites. *Compos. B Eng.* 1 (78), 174–184.
- Hamed, N., El-Feky, M.S., Kohail, M., Nasr, E.S., 2019. Effect of nano-clay deagglomeration on mechanical properties of concrete. *Constr. Build. Mater.* 30 (205), 245–256.
- Han, B., Ding, S., Wang, J., Ou, J. Nano-engineered cementitious composites: principles and practices. Springer Nature Singapore Pte Ltd., 2019, Page 731.
- Han, B., Li, Z., Zhang, L., Zeng, S., Yu, X., Han, B., Ou, J., 2017. Reactive powder concrete reinforced with nano SiO₂-coated TiO₂. *Constr. Build. Mater.* 1 (148), 104–112.
- He, X., Shi, X., 2008. Chloride permeability and microstructure of Portland cement mortars incorporating nanomaterials. *Transp. Res. Rec.* 2070 (1), 13–21.
- Heikal, M., Zaki, M.E., Ibrahim, S.M., 2021. Characterization, hydration, durability of nano-Fe₂O₃-composite cements subjected to sulphates and chlorides media. *Constr. Build. Mater.* 1, (269) 121310.
- Heikal, M., Ibrahim, N.S., 2016. Hydration, microstructure and phase composition of composite cements containing nano-clay. *Constr. Build. Mater.* 1 (112), 19–27.
- Herath, C., Gunasekara, C., Law, D.W., Setunge, S., 2020. Performance of high volume fly ash concrete incorporating additives: A systematic literature review. *Constr. Build. Mater.* 20, (258) 120606.
- Hosan, A., Shaikh, F.U., 2020. Influence of nano-CaCO₃ addition on the compressive strength and microstructure of high volume slag and high volume slag-fly ash blended pastes. *J. Build. Eng.* 1, (27) 100929.
- Hosan, A., Shaikh, F.U., 2021. Compressive strength development and durability properties of high volume slag and slag-fly ash blended concretes containing nano-CaCO₃. *J. Mater. Res. Technol.* 1 (10), 1310–1322.
- Hosan, A., Shaikh, F.U., Sarker, P., Aslani, F., 2021. Nano-and micro-scale characterisation of interfacial transition zone (ITZ) of high volume slag and slag-fly ash blended concretes containing nano SiO₂ and nano CaCO₃. *Constr. Build. Mater.* 1, (269) 121311.
- Huang, W. Clay nanopapers. *Nanopapers 2018 Jan 1* (pp. 59-86). William Andrew Publishing.
- Ibrahim, A.M. The effect of nano metakaolin material on some properties of concrete. *Diyala journal of engineering sciences.* 2013 Mar 1;6(1):50-61.
- Irshidat, M.R., Al-Saleh, M.H., 2018. Thermal performance and fire resistance of nanoclay modified cementitious materials. *Constr. Build. Mater.* 20 (159), 213–219.

- Jalal, M., Fathi, M., Farzad, M., 2013. Effects of fly ash and TiO₂ nanoparticles on rheological, mechanical, microstructural and thermal properties of high strength self compacting concrete. *Mech. Mater.* 15 (61), 11–27.
- Jiang, C.H., Zhou, C.S., Ji, H.B., Li, C.H., 2019. Research progress on the application of nano-metakaolin in cement-based materials. *Bull. Chin. Ceram. Soc.* 38, 3861–3867.
- Joshaghani, A., Balapour, M., Mashhadian, M., Ozbakkaloglu, T., 2020. Effects of nano-TiO₂, nano-Al₂O₃, and nano-Fe₂O₃ on rheology, mechanical and durability properties of self-consolidating concrete (SCC): An experimental study. *Constr. Build. Mater.* 10, (245) 118444.
- Kani, E.N., Rafiean, A.H., Alishah, A., Astani, S.H., Ghaffar, S.H., 2021. The effects of Nano-Fe₂O₃ on the mechanical, physical and microstructure of cementitious composites. *Constr. Build. Mater.* 10, (266) 121137.
- Karthikeyan, B., Dhinakaran, G., 2018. Influence of ultrafine TiO₂ and silica fume on performance of unreinforced and fiber reinforced concrete. *Constr. Build. Mater.* 10 (161), 570–576.
- Khosakhlagh, A., Nazari, A., Khalaj, G., 2012. Effects of Fe₂O₃ nanoparticles on water permeability and strength assessments of high strength self-compacting concrete. *J. Mater. Sci. Technol.* 28 (1), 73–82.
- Khotbehsara, M.M., Miyandehi, B.M., Naseri, F., Ozbakkaloglu, T., Jafari, F., Mohseni, E., 2018. Effect of SnO₂, ZrO₂, and CaCO₃ nanoparticles on water transport and durability properties of self-compacting mortar containing fly ash: Experimental observations and ANFIS predictions. *Constr. Build. Mater.* 15 (158), 823–834.
- Kumar, A., Oey, T., Kim, S., Thomas, D., Badran, S., Li, J., Fernandes, F., Neithalath, N., Sant, G., 2013. Simple methods to estimate the influence of limestone fillers on reaction and property evolution in cementitious materials. *Cem. Concr. Compos.* 1 (42), 20–29.
- Lee, S.J., Kawashima, S., Kim, K.J., Woo, S.K., Won, J.P., 2018. Shrinkage characteristics and strength recovery of nanomaterials-cement composites. *Compos. Struct.* 15 (202), 559–565.
- Liao, K.Y., Chang, P.K., Peng, Y.N., Yang, C.C., 2004. A study on characteristics of interfacial transition zone in concrete. *Cem. Concr. Res.* 34 (6), 977–989.
- Li, H., Zhang, M.H., Ou, J.P., 2006. Abrasion resistance of concrete containing nanoparticles for pavement. *Wear* 260 (11–12), 1262–1266.
- Li, H., Xiao, H.G., Yuan, J., Ou, J., 2004. Microstructure of cement mortar with nanoparticles. *Compos. B Eng.* 35 (2), 185–189.
- Li, W., Huang, Z., Zu, T., Shi, C., Duan, W.H., Shah, S.P., 2016. Influence of nanolimestone on the hydration, mechanical strength, and autogenous shrinkage of ultrahigh-performance concrete. *J. Mater. Civ. Eng.* 28 (1), 04015068.
- Li, G., Zhuang, Z., Lv, Y., Wang, K., Hui, D., 2020. Enhancing carbonation and chloride resistance of autoclaved concrete by incorporating nano-CaCO₃. *Nanotechnol. Rev.* 9 (1), 998–1008.
- Lin, Y., Chen, H., Chan, C.M., Wu, J., 2008. High impact toughness polypropylene/CaCO₃ nanocomposites and the toughening mechanism. *Macromolecules* 41 (23), 9204–9213.
- Li, W., Huang, Z., Cao, F., Sun, Z., Shah, S.P., 2015. Effects of nano-silica and nanolimestone on flowability and mechanical properties of ultra-high-performance concrete matrix. *Constr. Build. Mater.* 1 (95), 366–374.
- Liu, X., Chen, L., Liu, A., Wang, X., 2012. Effect of nano-CaCO₃ on properties of cement paste. *Energy Procedia* 1 (16), 991–996.
- Lothenbach, B., Le Saout, G., Gallucci, E., Scrivener, K., 2008. Influence of limestone on the hydration of Portland cements. *Cem. Concr. Res.* 38 (6), 848–860.
- Madandoust, R., Mohseni, E., Mousavi, S.Y., Namnevis, M., 2015. An experimental investigation on the durability of self-compacting mortar containing nano-SiO₂, nano-Fe₂O₃ and nano-CuO. *Constr. Build. Mater.* 1 (86), 44–50.
- Meng, T., Yu, Y., Qian, X., Zhan, S., Qian, K., 2012. Effect of nano-TiO₂ on the mechanical properties of cement mortar. *Constr. Build. Mater.* 1 (29), 241–245.
- Meng, J., Zhong, J., Xiao, H., Ou, J., 2021. Interfacial design of nano-TiO₂ modified fly ash-cement based low carbon composites. *Constr. Build. Mater.* 8, (270) 121470.
- Moro, C., Francioso, V., Schragar, M., Velay-Lizancos, M., 2020. TiO₂ nanoparticles influence on the environmental performance of natural and recycled mortars: A life cycle assessment. *Environ. Impact Assess. Rev.* 1, (84) 106430.
- Moreno-Maroto, J.M., Alonso-Azcárate, J., 2018. What is clay? A new definition of “clay” based on plasticity and its impact on the most widespread soil classification systems. *Appl. Clay Sci.* 1 (161), 57–63.
- Morsy, M.S., Al-Salloum, Y., Almusallam, T., Abbas, H., 2014. Effect of nano-metakaolin addition on the hydration characteristics of fly ash blended cement mortar. *J. Therm. Anal. Calorim.* 116 (2), 845–852.
- Nikbin, I.M., Mohebbi, R., Dezhampanah, S., Mehdipour, S., Mohammadi, R., Nejat, T., 2019. Gamma ray shielding properties of heavy-weight concrete containing Nano-TiO₂. *Radiat. Phys. Chem.* 1 (162), 157–167.
- Nazari, A., Riahi, S., Riahi, S., Shamekhi, S.F., Khademno, A., 2010. Benefits of Fe₂O₃ nanoparticles in concrete mixing matrix. *J. Am. Sci.* 6 (4), 102–106.
- Nazari, A., Riahi, S., 2011. Computer-aided design of the effects of Fe₂O₃ nanoparticles on split tensile strength and water permeability of high strength concrete. *Mater. Des.* 32 (7), 3966–3979.
- Ng, D.S., Paul, S.C., Anggraini, V., Kong, S.Y., Qureshi, T.S., Rodriguez, C.R., Liu, Q.F., Šavija, B., 2020. Influence of SiO₂, TiO₂ and Fe₂O₃ nanoparticles on the properties of fly ash blended cement mortars. *Constr. Build. Mater.* 20, (258) 119627.
- Nikbin, I.M., Mehdipour, S., Dezhampanah, S., Mohammadi, R., Mohebbi, R., Moghadam, H.H., Sadrmomtazi, A., 2020. Effect of high temperature on mechanical and gamma ray shielding properties of concrete containing nano-TiO₂. *Radiat. Phys. Chem.* 1, (174) 108967.
- Niu, X.J., Li, Q.B., Hu, Y., Tan, Y.S., Liu, C.F., 2021. Properties of cement-based materials incorporating nano-clay and calcined nano-clay: A review. *Constr. Build. Mater.* 17, (284) 122820.
- Norhasri, M.M., Hamidah, M.S., Fadzil, A.M., Megawati, O., 2016. Inclusion of nano metakaolin as additive in ultra high performance concrete (UHPC). *Constr. Build. Mater.* 30 (127), 167–175.
- Norhasri, M.M., Hamidah, M.S., Fadzil, A.M., 2017. Applications of using nano material in concrete: A review. *Constr. Build. Mater.* 15 (133), 91–97.
- Olutlu, M., Şahin, R., 2011. Single and combined effects of nano-SiO₂, nano-Al₂O₃ and nano-Fe₂O₃ powders on compressive strength and capillary permeability of cement mortar containing silica fume. *Mater. Sci. Eng., A* 528 (22–23), 7012–7019.
- Pera, J., Husson, S., Guilhot, B., 1999. Influence of finely ground limestone on cement hydration. *Cem. Concr. Compos.* 21 (2), 99–105.
- Paul, K.K., Giri, P.K., 2018. Plasmonic metal and semiconductor nanoparticle decorated TiO₂-based photocatalysts for solar light driven photocatalysis. *Encyclopedia of Interfacial Chemistry. Surface Science and Electrochemistry*, 786–794. <https://doi.org/10.1016/B978-0-12-409547-2.13176-2>.
- Pique, T.M., Vazquez, A., 2013. Control of hydration rate of polymer modified cements by the addition of organically modified montmorillonites. *Cem. Concr. Compos.* 1 (37), 54–60.
- Polat, R., Demirboğa, R., Khushefati, W.H., 2015. Effects of nano and micro size of CaO and MgO, nano-clay and expanded perlite aggregate on the autogenous shrinkage of mortar. *Constr. Build. Mater.* 15 (81), 268–275.
- Praveenkumar, T.R., Vijayalakshmi, M.M., Meddah, M.S., 2019. Strengths and durability performances of blended cement concrete with TiO₂ nanoparticles and rice husk ash. *Constr. Build. Mater.* 30 (217), 343–351.
- Rao, S., Silva, P., De Brito, J., 2015. Experimental study of the mechanical properties and durability of self-compacting mortars with nano materials (SiO₂ and TiO₂). *Constr. Build. Mater.* 15 (96), 508–517.
- Ren, J., Lai, Y., Gao, J., 2018. Exploring the influence of SiO₂ and TiO₂ nanoparticles on the mechanical properties of concrete. *Constr. Build. Mater.* 30 (175), 277–285.
- Ren, Z., Liu, Y., Yuan, L., Luan, C., Wang, J., Cheng, X., Zhou, Z., 2021. Optimizing the content of nano-SiO₂, nano-TiO₂ and nano-CaCO₃ in Portland cement paste by response surface methodology. *J. Build. Eng.* 1, (35) 102073.
- Sadeghi-Nik, A., Berenjian, J., Bahari, A., Safaei, A.S., Dehestani, M., 2017. Modification of microstructure and mechanical properties of cement by nanoparticles through a sustainable development approach. *Constr. Build. Mater.* 30 (155), 880–891.
- Salih, A., Rafiq, S., Mahmood, W., Hind, A.D., Noaman, R., Ghafor, K., Qadir, W., 2020. Systemic multi-scale approaches to predict the flowability at various temperature and mechanical properties of cement paste modified with nano-calcium carbonate. *Constr. Build. Mater.* 30, (262) 120777.
- Sanchez, F., Sobolev, K., 2010. Nanotechnology in concrete—a review. *Constr. Build. Mater.* 24 (11), 2060–2071.
- Sanalkumar, K.U., Yang, E.H., 2021. Self-cleaning performance of nano-TiO₂ modified metakaolin-based geopolymers. *Cem. Concr. Compos.* 1, (115) 103847.
- Shaikh, F.U., Supit, S.W., 2014. Mechanical and durability properties of high volume fly ash (HVFA) concrete containing calcium carbonate (CaCO₃) nanoparticles. *Constr. Build. Mater.* 15 (70), 309–321.
- Shaikh, F.U., Supit, S.W., 2015. Chloride induced corrosion durability of high volume fly ash concretes containing nano particles. *Constr. Build. Mater.* 30 (99), 208–225.
- Shchelokova, E.A., Tyukavkina, V.V., Tsyryatyeva, A.V., Kasikov, A.G., 2021. Synthesis and characterization of SiO₂-TiO₂ nanoparticles and their effect on the strength of self-cleaning cement composites. *Constr. Build. Mater.* 10, (283) 122769.
- Shebl, S., Allie, L., Morsy, M., Aglan, H.A., 2009. Mechanical behavior of activated nano silicate filled cement binders. *J. Mater. Sci.* 44 (6), 1600–1606.
- Sikora, P., Cendrowski, K., Markowska-Szczupak, A., Horszczaruk, E., Mijowska, E., 2017. The effects of silica/titania nanocomposite on the mechanical and bactericidal properties of cement mortars. *Constr. Build. Mater.* 30 (150), 738–746.
- Sorathiya, J., Shah, S., Kacha, S.M., 2017. Effect on addition of nano “titanium dioxide”(TiO₂) on compressive strength of cementitious concrete. *Kalpa Publications in Civil Engineering.* 22 (1), 219–225.
- Souza, D.A., Araujo, D.M., Carvalho, C.D., Yoshida, M.I. Physico-chemical analysis of flexible polyurethane foams containing commercial calcium carbonate. *Materials research.* 2008 Dec;11(4):433-8.
- Su, Y., Li, J., Wu, C., Wu, P., Li, Z.X., 2016. Influences of nano-particles on dynamic strength of ultra-high performance concrete. *Compos. B Eng.* 15 (91), 595–609.
- Sun, J., Xu, K., Shi, C., Ma, J., Li, W., Shen, X., 2017. Influence of core/shell TiO₂-SiO₂ nanoparticles on cement hydration. *Constr. Build. Mater.* 156, 114–122.
- Sun, Y., Zhang, P., Guo, W., Bao, J., Qu, C., 2020a. Effect of nano-CaCO₃ on the mechanical properties and durability of concrete incorporating fly Ash. *Adv. Mater. Sci. Eng.* 2020, 1–10.
- Sumesh, M., Alengaram, U.J., Jumaat, M.Z., Mo, K.H., Alnahhal, M.F., 2017. Incorporation of nano-materials in cement composite and geopolymer based paste and mortar—A review. *Constr. Build. Mater.* 1 (148), 62–84.
- Ulkeryildiz, E., Kilic, S., Ozdemir, E., 2016. Rice-like hollow nano-CaCO₃ synthesis. *J. Cryst. Growth* 15 (450), 174–180.
- Varga, G., 2007. The structure of kaolinite and metakaolinite. *Epitoanyag.* 59 (1), 6–9.
- Wu Z, Khayat KH, Shi C, Tutikian BF, Chen Q. Mechanisms underlying the strength enhancement of UHPC modified with nano-SiO₂ and nano-CaCO₃. *Cement and Concrete Composites.* 2021 Feb 27:103992.
- Wu, Z., Shi, C., Khayat, K.H., Wan, S., 2016. Effects of different nanomaterials on hardening and performance of ultra-high strength concrete (UHSC). *Cem. Concr. Compos.* 1 (70), 24–34.

- Wu, Z., Shi, C., Khayat, K.H., 2018. Multi-scale investigation of microstructure, fiber pullout behavior, and mechanical properties of ultra-high performance concrete with nano-CaCO₃ particles. *Cem. Concr. Compos.* 1 (86), 255–265.
- Xu, Y., Jin, R., Hu, L., Li, B., Chen, W., Shen, J., Wu, P., Fang, J., 2020. Studying the mix design and investigating the photocatalytic performance of pervious concrete containing TiO₂-Soaked recycled aggregates. *J. Cleaner Prod.* 1, (248) 119281.
- Yang, H., Yan, Y., Hu, Z., 2020. The preparation of nano calcium carbonate and calcium silicate hardening accelerator from marble waste by nitric acid treatment and study of early strength effect of calcium silicate on C30 concrete. *J. Build. Eng.* 1, (32) 101507.
- Zhang, S.L., Qi, X.Q., Guo, S.Y., Ren, J., Chen, J.C., Chi, B., Wang, X.C., 2021. Effect of a novel hybrid TiO₂-graphene composite on enhancing mechanical and durability characteristics of alkali-activated slag mortar. *Constr. Build. Mater.* 15, (275) 122154.
- Zhang, R., Cheng, X., Hou, P., Ye, Z., 2015. Influences of nano-TiO₂ on the properties of cement-based materials: Hydration and drying shrinkage. *Constr. Build. Mater.* 15 (81), 35–41.
- Zhan, P.M., He, Z.H., Ma, Z.M., Liang, C.F., Zhang, X.X., Abreham, A.A., Shi, J.Y., 2020. Utilization of nano-metakaolin in concrete: A review. *J. Build. Eng.* 1, (30) 101259.